ORKUSTOFNUN
NATIONAL ENERGY AUTHORITY

THE UNITED NATIONS UNIVERSITY

GEOPHYSICAL LOGGING IN WELL SG-9, SVARTSENGI GEOTHERMAL FIELD, SW-ICELAND

J. Luis Zúniga

UNU Geothermal Training Programme, Iceland.

Report 1980-8

GEOPHYSCAL LOGGING IN WELL SG - 9, SVARTSENGI GEOTHERMAL FIELD, SW-ICELAND

J. Luis Zuniga [+],
UNU Geothermal Training Programme,
National Energy Authority,
Grensásvegur 9, 108 Reykjavik,
Iceland

[+] Permanent address:
Comisión Ejecutiva Hidroelectrica
del Rio Lempa,
Superintendencia de Recursos
Geotermicos,
Centro de Goblerno, San Salvador,
El Salvador - Centro America

ABSTRACT

Interpretation of various geophysical logs from the 994 m deep well SG-9 in the Svartsengi high temperature geothermal field in SW-Iceland, shows fairly good agreement with the local geology of the area, and other wells drilled in this field. The average value of SiO_2 of the rocks penetrated by the hole, obtained by the natural gamma ray log, is 48.9%, which is in good agreement with the average value of 48.23% reported by Jakobsson et al. (1978) for lavas in the area. The porosity of the rocks is generally found to be high with porosity values ranging from 5% to approximately 40%. The bulk density is found to be in the range of 2.5-3.0 g/cm^3, but generally the density is fairly constant along the well. The resistivity is found to be in the range 1-160 Ωm, with the lower values being caused by the high porosity and the salinity of the reservoir fluid. The diameter of the well shows considerable variations, and cavities up to 29" in diameter, are recorded (the bit diameter used at that spot is 17 1/2"). It is found that the changes in the self potential and the differential temperature are in some cases related to the cavities. The differential temperature log is found to be a powerful tool to locate aquifers in the well, and the aquifers are predominantly located where cavities are recorded by the caliper log.

LIST OF CONTENTS

LIST OF FIGURES

15 - Log response at different time constants and same logging speed

16 - Log response at two different time constants and two different logging speeds

17 - Relation between natural gamma ray intensity and SiO_2, IRDP hole, Áreyjar, Reydarfjördur

18 - Absorption function of the borehole fluid

19 - Behaviour of the anomaly from a semi infinite radioactive layer

20 - Influence of the borehole radius R on the shape of the semi infinite anomaly F (Z)

21 - Influence of the detector length L on the shape of the semi infinite anomaly

22 - Influence of the layer thickness on the shape of the radioactive anomaly

23 - Compton scattering

24 - Photoelectric effect

25 - Pair production

26 - Gamma-ray response for cased and uncased wells

27 - Neutron-neutron log response versus hole size and porosity

28 - Calibration curves for gamma-gamma log

29 - Sheets 1, 2, 3 and 4 geophysical logs and geological section of well SG-9

LIST OF TABLES

1 INTRODUCTION

1.1 Scope of work

The writer was awarded a UNU Fellowship to attend the 1980 Geothermal Training Programme at the National Energy Authority of Iceland, supported by the United Nations University, and the Government of Iceland.

The course started with basic introductory lectures and field work. After the first four weeks of general aspects in geothermal studies, the author received specialized training in borehole geophysics, mainly oriented to the application of nuclear logging for lithologic studies.

The training was divided in lectures given by specialists of N.E.A. and four weeks of field work. The training programme also included a two weeks geothermal excursion around Iceland. The work for the present report was accomplished in the last nine weeks of the training.

The principal techniques being applied by the author in the study of well SG-9 presented here are the 16" and 64" resistivity logs, gamma ray log (natural radioactivity of the formations), neutron-neutron log (porosity determination of the formations), and gamma-gamma log (density of the formation). However,a total of eleven physical parameters were measured in the well.

1.2 The Svartsengi geothermal field

Well SG-9 is a 994 m deep drillhole in the Svartsengi high temperature geothermal field, located in the Reykjanes peninsula in SW Iceland.

This field is exploited for space heating of five villages on the Reykjanes peninsula, and has an installed capacity of 100 Mw_t . A small electrical power unit of 2 Mw_e using the geothermal steam, is also built in the plant (Thorhallsson, 1979).

Detailed surface and subsurface investigations have been conducted in this area in recent years.

Surface studies

Geological, geophysical and geochemical studies, have been performed to locate the field, and its boundaries.

Prior to drilling the only surface thermal manifestations were minor amount of steam rising through fresh recent lava flows (Jonsson, 1978).

The surface geology shows that all the Reykjanes peninsula is composed by basaltic formations without any evidence of acidic or intermediate units. The geothermal activity of the Svartsengi field is controlled by fissures and faults as the field is set in the middle of a belt of tectonic and volcanic activity (Fig. 1).

The main geophysical exploration method used in the Svartsengi geothermal field, is electrical resistivity soundings. The resistivity measurements indicate a horizontal extension of the field as 5 km^2 at 200 m depth and it increases to 7 km^2 at 600m below sea level (Georgsson, 1979). This extension refers to the 5 Ωm contour line (Fig. 2).

The composition of geothermal water shows relatively high salinity in the geothermal fluid. Chemical analyses of the geothermal water indicate about 67% seawater, but deuterium measurements give only about 57% sea water (Arnason, 1977). It is assumed that the geothermal water is affected by seawater mixed with fresh water.

Sub-surface studies

The borehole geology has been studied in detail in the wells drilled in the field and geophysical logs have been performed in some of the wells.

The borehole geology studies are done by examination of the cuttings sampled every two meters when the well is drilled. These studies consist of petrological studies, thin section examinations and X-ray analyses. The results show a fairly uniform picture of the geological conditions in the geothermal reservoir, with alternating layers of basaltic lavas and hyaloclastites.

In borehole geophysics, eleven different geophysical parameters are now normally measured in geothermal wells in Iceland. However, only few wells in Svartsengi have been investigated by these methods.

The lithological logs show that the reservoir in Svartsengi has a high porosity, and is formed by basic formations. No acidic or intermediate layers have been detected so far. This is in agreement with the results of borehole geology and the surface geological investigations (Franzson, pers. comm., Jonsson,1978, Jakobsson et al. 1978).

2 GEOPHYSICAL LOGS - METHODS AND TECHNIQUES

2.1 Introduction

Geophysical logs, other than pressure and temperature logs, are new in geothermal investigation. Techniques developed in the oil industry are being adapted for this purpose. Due to the different geological environments in geothermal and oil fields, many concepts must be modified for a proper use of these methods. The responses of volcanic rocks, where the geothermal areas are normally situated are quite different from the sedimentary environment of the oil fields.

Until recently the lithological studies in geothermal exploration have mainly been done by studies of cores and cuttings recovered during the drilling. In geophysical logging, physical parameters related to the properties of the rocks penetrated by drilling are measured. Such studies

can provide continuous objective records, which are consistent and independent of environment and time, if the logs are properly calibrated.

This report presents a brief description of some of the geophysical logging methods used in geothermal areas in Iceland, and a qualitative interpretation is applied to well SG-9 in the Svartsengi field. Due to the early stage of the applications of these methods in geothermal exploration, only a qualitative interpretation is available at present. However, fairly good results are obtained in the detection of changes in formations, bed thicknesses, resistivities, porosities and densities of the formations penetrated by this particular well.

2.2 Caliper logs

The caliper log is performed to obtain knowledge on the average diameter of the well. It is run in cased wells in order to get information on the state of the casing and in open holes to locate cavities in the walls.

The caliper log is run by a probe on which three movable arms are placed (Fig. 3). The arms can be opened or closed by an electric motor placed within the tool, but which is controlled on the surface. The arms continuously record the diameter of the well by following the walls of the hole. The signal is sent to the surface as pulses of different frequencies, which are continuously recorded by electronic equipment.

The calibration of the tool is made before and after the instrument is placed in the hole. It is done by placing the tool in a hole of a board which has several smaller holes at different distances from the probe. The signal obtained as the arms are placed in different holes corresponds to different diameters of the hole. The effect of temperature on the response of the tool is not negligible. Therefore, the calibration is performed both, before and after each log. Usually the latter calibration is more reliable.

The hole diameter is by no means as uniform as the drill bit is supposed to drill the hole. This is due to a combination of drilling technique problems and the lithology of the formations. A soft formation will show less resistance to be drilled than the hard one, and soft formations seem to be more prone to form cavities. The caliper log can be used for

location of lithological boundaries and thus for statigraphic correlations. It can also be used for the detection of fractures and cavities and can be a guide for well construction. However, its most important use in geophysical logging is the detailed information on well diameter, which can be used for the correction of the values obtained by the other geophysical logs, especially the nuclear logs.

2.3 Temperature logs

The temperature logs are recorded in two ways, i.e. the absolute temperature and the differential temperature.

Absolute temperature can be recorded both by using mechanical tools as well as electronic ones. In geothermal exploration mechanical instruments are used at high temperatures. Electronic equipment can at present only be used in temperatures up to 180°C. The mechanical tools are of burdon tube type (Amerada gauge) which records the boiling pressure of a special fluid, and of bimetal type (Kuster gauge) where the temperature expansion of the bimetal is recorded (Stefansson & Steingrímsson, 1980). The mechanical tools do not transmit the data to the surface, but data are recorded on a chart placed inside the tool on a clock driven recorder. These instruments have an accuracy of ± 1°C. The electronic tools for temperature measurements have better sensitivity than the mechanical ones, but their application is limited to temperatures below 180°C. They are used in low temperature areas or during the drilling period, when the hole is cooled by the drilling fluid. The principle with which these tools work, is the relation of resistivity with temperature. This is done by placing the sensor, a platinum thermometer or thermistor, at the lower end of an electrical cable, which transmits the signal to the recording equipment on the surface. The signal can be measured directly as the resistivity or by coupling the sensor into a resonant circuit, where the temperature is related with the frequency of the pulses transmitted to the surface (Stefansson & Steingrímsson, 1980).

The differential temperature log, like its name suggests, records the differences or changes in temperature occurring within the borehole. The values, which are referred to as positive or negative, are useful to detect inflow and outflow zones in the formations traversed by the hole. Due to the high sensitivity of the tool, a clear response is recorded where aquifers are located in wells.

2.4 Cement bond logs

This log is used to obtain information on the conditions of the cement behind the casing. The cementation job has the purpose to fix the casing against the walls of the hole, but also to protect the migration of fluids from one formation to another.

It has been found that when a single-detector continuous velocity log is run in a well, the path of minimum travel time for the acoustic wave between the transmitter and the detector is through the wall of the well (Willie, 1963). The principle of this method is to measure the amplitude of the sonic wave which has travelled along the wall of the well with the characteristic speed of a sonic wave in iron, which has higher velocity in iron than in most rocks or cement. The amplitude of an arriving wave at a given time is registered. If the casing is uncemented in the well, the amplitude of the wave corresponding to the velocity in iron is high. If the casing is well cemented to the walls of the well, the amplitude of the wave travelling with the velocity of sound in iron, is attenuated to almost zero value. The degree of cementation is in this way the relative amplitude of the sound wave with the velocity of 5.9 km/s , which is the velocity of the sound in iron.

The probe containing the wave transmitter and the receiver is placed down hole, and the signal is sent through an electrical cable to the surface where is registered by electronic devices.

2.5 Resistivity logs

The Ohm's law, one of the basic concepts in the theory of electricity, states that the amount of current (I) through a conductor is proportional to the difference in potential (V) caused by the flow and a constant of proportionality, which is the opposition of the conductor to transport the flow of current. This opposition is called resistance and is expressed by the Ohm's law in the form:

$$R = \frac{V}{I} \qquad (1)$$

where:

R = the resistance to the flow of current (ohms)

V = difference of potential (volts)

I = electrical current (ampers)

The resistance depends on the nature of the conductor, the cross section area and the length of the conductor. The length of the current path and the cross section area of a conductor, can be taken into account in order to obtain a property that depends not on the dimensions of the conductor but only on its nature. This property is called resistivity or specific resistance, and it is expressed by the formula:

$$\gamma = \frac{RA}{L} \qquad (2)$$

where:

γ = resistivity in Ohm m^2/m or Ωm

R = resistance in Ohm

A = area in m^2

L = length in m

Resistivity can be defined as the resistance between the opposite faces of a cube of a conductor, which is one meter on each side.

One of the electrical logs, the resistivity log, is performed to measure this property along the formations in the borehole. The resistivity depends on the physical properties of the rocks and on the properties of the fluids contained in the rocks. In water bearing rocks, the resistivity will depend on the amount of water present, salinity of the water and the form in which the water is distributed in the formations (Keller and Frischknect, 1966). When a saline solution is present in the rock, the resistivity of the formation can be described by taking into account the electrical properties of an electrolite. In saline solutions the ions are free to move independently. Where an electrical current is applied through the solution, these ions are acelerated, the cations to the positive pole and the anions to the negative pole. The current will depend on the amount of ions present in the solution. In viscous solutions the current depends on temperature. By increasing the temperature of the solution and decreasing its viscosity the ions obtain higher mobility, which is equvalent to lower resistivity.

The dependence of resistivity on the temperature of rocks saturated with electrolites is given by the equation:

$$\gamma_t = \frac{\gamma\ (t_o)}{1 + \alpha\ (t - t_o)} \qquad (3)$$

(Keller and Frischknecht, 1966)

where:

$\gamma_{(t)}$ = resistivity at temperature t

$\gamma_{(t_o)}$ = resistivity at a reference temperature

α = temperature coefficient of resistivity ($\simeq$ o.o25/°C for most electrolites)

t = ambient temperature °C

t_o = reference temperature °C

Since groundwater usually contains variety of salt in solution, it is hard to compute the salinity from chemical analyse. Hence a concept of equivalent salinity is used to discuss the resistivity of groundwater. This concept is defined as the salinity of a sodium chloride solution which would have the same resistivity as that of a particular solution for which the equivalent salinity is being expressed (Keller and Frishknecht, 1966).

Fig. 4 shows the resistivity of solutions of sodium chloride as a function of concentration and temperature. Fig. 5 shows relationships between the resistivity and the concentration of various salt solutions at a reference temperature of 18°C.

The resistivity measured in a borehole is not the resistivity of the rock itself, but the resistivity of the mixture of rock and water. The value is the γ_o or total resistivity. The resistivity of the water γ_w and the true resistivity of the rock can be calculated through the relation

$$\gamma_w = \frac{\gamma_o}{F} \qquad (4)$$

where F is the formation factor and is defined as the ratio of the electrical resistivity of a rock saturated with water to the resistivity of the water with which it is saturated (Archie, 1942). This factor is ralated to the porosity of sedimentary rocks. From data on porosity and resistivity it has been possible to determine the relation between salinity, porosity and resistivity in sedimentary rocks, as shown in fig. 6 .

For most of rocks the conduction of electrical current is entirely through the water contained in the pores of the rock. Thus the resistivity of the rocks is related to the porosity of the rocks, and depends on how the water is distributed in the formation. Related to the pore

geometry, rocks can be grouped in three general categories: (1) Intergranular porosity, consisting of the pore space left over after the rocks grains were compacted. (2) Joint porosity, occurring particulary in igneous rocks. (3) Vug porosity, consisting in large irregular cavities. In these three types of porosity, the pore volume may be divided in two parts: the storage pores, which are large voids and the finer connecting pores.

In all rocks the three types of porosity are usually present but in different proportions (Keller and Frischknecht, 1966).

The ranges of porosity to be expected in rocks are shown in Table 1.

Table 1 Normal ranges in porosity for rocks (From Keller and Frischknecht, 1966)

Rock type	Intergranular porosity (%)	Joint porosity (%)	Vug porosity* (%)
Paleozoic sandstones and shales	5-30	0-1	0
Paleozoic limestones	2-10	0-2	0
Paleozoic clastic volcanics	5-30	0-2	0
Post-Paleozoic sandstones and shale	10-40	0	0
Post-Paleozoic limestones	4-20	0-2	0
Post-Paleozoic clastic volcanics	10-60	0	0
Precambrian sediments and low-rank metamorphosed sediments	1-8	0-2	0
Precambrian igneous rocks and high-rank metamorphic rocks	0-2	0-2	0
More recent igneous rocks	0-10	0-2	0

*Vug porosity accounts for an appreciable total porosity in rare cases.

Resistivity logging is performed to measure the electrical resistivity of a volume of earth material, when an electrical current is applied. Resistivity devices can be applied to determine parameters such as the formation resistivity, formation porosity, mud cake resistivity, invaded zone resistivity and porosity, hydrocarbon and water saturation, fluid

resistivity, formation factor and correlation with geological formations (Keys and Mac Cary, 1971).

The measurement of resistivity in a borehole is similar to the measurement of resistivity of cores in a laboratory, or the measurement of resistivity in surface exploration. The similarity of resistivity measurements in both cores and boreholes is shown in fig. 7.
In the core measurements the resistivity of the sample is the resistivity given by formula (5)

$$\gamma_T = \frac{V}{I} \times \frac{S}{L} \qquad (5)$$

where the ratio between the cross section area and the length of the sample(called the geometrical factor G) can be simplified by predetermining these parameters. In the borehole this procedure is not usable, where the resistivity is measured along the formations penetrated by the hole, and the current flow lines are not confined to a cylindrical shape. Thus the geometrical factor G is not a simple ratio of length and area.

Due to the effect of the new geometrical factor and the current distortion by the fluid filling the borehole, the results obtained give the apparent resistivity measured over an average of a certain volume of the rocks surrounding the probe. This apparent resistivity is given by the formula:

$$\rho = \frac{V}{I} \times G \qquad (6)$$

which represents the same relation as (5), but where the values of G must be calculated for each logging device from the arrangement of the electrodes and their spacing.

There are many types of instrumental techniques for recording resistivity logs, but only the normal resistivity device,which is the log recorded for this study, will be discussed.

In the application of normal logs a four electrode array is used. Two electrodes are situated in the probe, which is placed in the well on the end of a multiconductor cable. The electrodes not fixed in the probe are placed far away from the set of electrodes in the probe, one

on the surface and the other one is the armor of the cable. The current is driven between an inhole electrode A and a electrode B located approximately 30 m above the probe. One current electrode and one potential electrode are fixed on the probe. There are two kinds of normal logs, the short normal log where the potential electrode M is placed at 16" distance from the A current electrode, and the long normal log where the M electrode is placed at 64" distance from the current electrode. The other potential electrode N is situated at surface. Both arrays, short and long normal are shown in fig. 8.

Measuring the apparent resistivity of the rocks surrounding the electrodes, the short normal logs,give a good vertical resolution, but the apparent resistivity measured is usually lower than the true resistivity. On the other hand, the long normal log records the apparent resistivity of the rocks beyond the invaded zone and the values are closer to the true resistivity of the rocks.The resolution of the long normal log is less than that of the short normal log.

The distance between the two electrodes A and M fixed in the probe is called spacing. These two electrodes are relatively close together but the distance of the electrodes B and N from the probe is considered to be electrically infinite. The distance AB should be at least twelve times the distance AM.

An electric current of a known value is sent between the electrodes A and B. The medium around A is assumed to be infinite, homogeneous and isotropic. The current lines from A are supposed to flow radially in all directions. It is possible to find the potential at any given point of equal distance from A so that all the current lines have the same intensity. The region that contributes most of the signal is a sphere of twice the diameter of the spacing AM, with its centre in the mid point of this spacing, called the reference point. The equipotential surfaces in form of spheres determine the potential at the electrode M, see Fig. 9.

Referring to Ohm's law, we know that the potential is represented by the formula (1)

$$V = IR$$

and by (2), we know the resistance:

$$R = \gamma \frac{L}{A}$$

and from (6) where $L/A = G$, we have:

$$V = I \gamma G \qquad (7)$$

where G is the geometrical factor and its value depends on the electrode spacing.

In fig. 9 the voltage measured on the surface of thickness dr , of the equipotential spheres, at M is dV , relating these concepts to (5) and (7) , we obtain:

$$dV = I \gamma \frac{dr}{4\pi r^2} \qquad (8)$$

where:

$4\pi r^2$ = area of sphere

dr = thickness of surface

r = radius of sphere.

Since r is equal to the distance AM , the summation of equipotential spheres from r to the electrode N at infinite is:

$$dV = \int_{AM}^{AN} I\gamma \frac{dr}{4\pi r^2}$$

$$= \frac{I\gamma}{4\pi} \int_{AM}^{AN} \frac{dr}{r^2}$$

$$= \frac{I\gamma}{4\pi} \left[- \frac{1}{r} \right]_{AM}^{AN}$$

$$= \frac{I\gamma}{4\pi} \left(\frac{1}{AM} - \frac{1}{AN} \right)$$

Considering N placed in the infinite, the term $\frac{1}{AN} = 0$

and $$V = \frac{I \gamma}{4\pi\ AM} \qquad (9)$$

The potential reading at M electrode is related to resistivity by equation (9), where

V = measured potential

γ = resistivity

I = electrical current used in the log

AM = electrode spacing.

From equation (9) we obtain the resistivity:

$$\gamma = 4\pi \, AM \, \frac{V}{I} \qquad (10)$$

As this is not the true resistivity, but the apparent resistivity we have to distinguish between the two concepts and we rewrite the equation:

$$\rho = 4\pi \, AM \, \frac{V}{I} \qquad (11)$$

where 4π AM is the geometrical factor.

If the B electrode is located at a distance which is considered finite, G will be influenced by B and we do not have a normal electrode array but a three electrode arrangement.

The two normals, short and long, are run at the same time in this measurement.

The logging equipment used in this study is manufactured by Gearhart-Owen, and the logs are run on a four conductor cable. Two conductors are used to send the electrical current to the electrodes A and B , and the other two are connected to the 16" and 64" potentials electrodes.

The current electrode A is placed in the probe together with the 16" and 64" potential electrodes M_1 and M_2 , the B current electrode is the armor of the cable isolated 30 m upwards from the probe. The reference potential electrode N is placed at the surface in a mud pit and needs good contact with the earth. The measured values are recorded continuously by electronic equipment on the surface.

The normal devices, like other electrical methods which measure apparent resistivity, are calibrated in Ohm-m. Normally the calibration is done by a calibration box supplied by the manufacturer of the equipment.

2.6 Self potential logs

The self potential or spontaneous potential log is a record of the electromotive forces between a fixed point at the surface and a movable point in

the borehole. By definition the electric potential is the measure of the potential from one point to another. Absolute zero has no meaning since we are only measuring the changes between two points.

The spontaneous potential log is a record of small differences of voltage, measured in millivolts, and is associated with the formations. It is caused by the borehole fluid, the shale of clay component and the water in the aquifers (Keys and Mac Cary, 1971). This potential is mainly attributed to electrochemical or electromotive sources.

These electromotive forces are produced in the junction of dissimilar materials in the borehole (Keys and Mac Cary, 1971). When two sodium chloride solutions of different concentration are separated by a permeable wall, causing the migration of ions from the more concentrated solution to the dilute one, and connected by an external conductor, an electrical current flows between the two solutions through the conductor. Depending on the degree of permeability of the wall, these effects are called shale potential or liquid junction potential (Fig. 10).

A similar situation occurs between shale and permeable beds which are penetrated by the hole, filled by a conductive fluid. Fig. 11 shows this situation in which it is assumed that both mud and water in the permeable bed contain only sodium chloride in solution and the water in the permeable bed is more saline than the mud.

The electrokinetic potential force is developed when an electrolite is moved through a permeable medium. In a borehole this potential can appear when drilling fluid is passing through permeable layers in zones where there is inflow or outflow in the borehole. This effect can occur if there is a differential pressure between the formation fluid and the drilling fluid. Also the layers in which this appears must be permeable. If the hydrostatic pressure of the fluid in the borehole is equal to the formation pressure, the electrokinetic potential is zero.

Taking in account the sources of the self potential it can be used for:

a. correlation and sub-surface mapping

b. determination of bed thickness

c. determination of formation water salinity.

The self potential (S.P.) curve is recorded placing a probe with an electrode into the borehole and the other electrode in a mud pit at the surface. Normally it is recorded together with the normal resistivity log, using the 16" potential electrode also for the S.P. response. The device to record the potential is a millivolt-meter. The electrode placed in the borehole records the drop of potential caused by the current flowing along the formations or from the hole and into the formations. Since one of the electrodes is placed at the surface, where the potential remains constant, the measured potential represents the change in potential along the borehole.

The self potential is usually measured in millivolts. The scale used depends on the changes expected, normally the scale 1 cm = 10 mV is used. Since the S.P. curve records only the changes in potential and not the absolute values, absolute zero has no meaning.

The main factors affecting the S.P. curves are:

1. Bed thickness
2. Resistivity of the bed
3. Salinity of the drilling fluid
4. Diameter of the well
5. Hydrostatic pressure of drilling fluid column

Fig. 12 shows examples of S.P. curves affected by some of the parameters mentioned above.

2.7 Nuclear logs

The nuclear logs are well known in oil exploration, and have recently been introduced in geothermal investigations. The response of volcanic rocks to nuclear logs and the interpretation of such data is a young discipline and is still in a development stage.

Included in this report are the natural gamma ray log, neutron-neutron and gamma-gamma logs, which are the simplest types of nuclear logs. In the oil industry pulsed neutron logs have been found valuable. The technique used in nuclear logging has developed to a certain degree of standardization. In the earlier years, each logging company used

their own methods of calibration, until common units were introduced by the American Petroleum Institute. These API units are the API gamma ray unit for the natural gamma ray log, and the API neutron unit for the neutron-neutron log.

The natural gamma ray is performed to measure the natural radioactivity of the rocks. The neutron-neutron log measures the porosity of the formations. The gamma-gamma log shows the bulk density of the formations penetrated by the borehole. All of these methods can be used in open or cased holes filled with any kind of fluid. Since the response of the logs depends on the nature of the rocks, the thickness of the layers, the time constant of the measuring system, and the logging speed, it is necessary to select proper values for these parameters in accordance with the demand on accuracy and resolution of the logs as well as the time available for the logging operation.

2.7.1 Performance of nuclear logs

The information gained in all nuclear logs depend on the counting rate recorded. The resolution and accuracy of the log depends on the logging speed and the time constant selected for the ratemeter. The following treatment is based on the lecture notes of Czubek (1978). The ratemeter time constant, which we simply will call time constant, is chosen depending on the accuracy we want to obtain, the logging speed we are going to use, or both. If we have no limitation on the time to spend to run the log, the time constant ($R\,C$) will depend only on the accuracy needed. The time constant is the interval of time in which the pulses from the detector of the probe are counted. The quantity of pulses per time unit is called intensity (I). When a log is run and the intensity along the borehole is not constant we call $I(t)$ the variable intensity and the influence of the logging speed has to be considered. The relation between the logging speed (V) the time (t) and the depth (z) along the borehole is $z = t \cdot V$. When the intensity along the borehole is registered on the recorder, the value obtained depends on the time constant and the logging speed. This value, called the dynamic anomaly ($J(t)$), is different from the true value of the formation intensities, which is called static anomaly ($I(z)$). The value of $J(z)$ will be close to $I(z)$, if we let the probe register as much counts as possible from the formation. That means a low logging speed. Therefore

we can have a different logging speed depending on the ratemeter time constant selected.

For the case of logging, the different anomalies are represented by the equations:

$$J(z) = \frac{1}{V \cdot RC} \; e^{-\frac{z}{VRC}} \int_{-\infty}^{z} I(z^1) \; e^{\frac{z^1}{VRC}} \; dz^1 \qquad (13)$$

and $$I(z) = J(z) + VRC \frac{dJ(z)}{dz} \qquad (14)$$

(Czubek, 1978)

and are represented by fig. 13.

Relating the areas under both curves we obtain:

$$S = \int_{-\infty}^{+\infty} I(z)\, dz = \int_{-\infty}^{+\infty} J(z)\, dz \qquad (15)$$

(Czubek, 1978)

We can suppose a rectangular form for the static anomaly having:

$$I_z = \begin{cases} 0 & z \leq 0 \\ I & 0 \leq Z \leq H \\ 0 & z \geq H \end{cases}$$

where H = thickness of the layer

Taking equations (13) for this case, we obtain:

$$J(z) = \begin{cases} 0 & Z \leq 0 \\ I \; (1-e^{-\frac{z}{VRC}}) & 0 \leq Z \leq H \\ I \; (1-e^{-\frac{H}{VRC}}) \cdot e^{-\frac{Z-H}{VRC}} & Z \geq H \end{cases}$$

(Czubek, 1978)

which is represented in fig. 14.

We can see that the maximum value for J(z) is when Z = H , then the relation for J(z) when Z = H is

$$J(H) = I\ (1-e^{-\frac{H}{VRC}}) \qquad (16)$$

(Czubek, 1978)

and the value for I(z) = I is higher than J(z) by I-J(H). This difference, which we want to have as small as possible is called the dynamic distortion is equal to:

$$\Delta = \frac{I - J(H)}{I} = e^{-\frac{H}{VRC}} \qquad (17)$$

For qualitative purposes this difference is usually taken as 5%, but must for quantitative analyses be smaller. By (17), we can calculate the time related to R C which the probe needs to be inside the layer to record the maximum value of the dynamic anomaly. Table 2 shows the relation between dynamic distortion and the time related to R C

We can see from Table 2, that the time required for the probe to be inside the layer for qualitative measurements is almost equal to three times R C , and must for quantitative measurements be higher than this value. From this we can select the value of the factor VRC to be used in terms of the thickness of the layer we want to investigate.

Once the value VRC is selected, the next step is to divide the values of the logging speed (V) and the time constant (R C). If the value of R C is chosen first, according to the accuracy needed, the value of V is obtained from the VRC relation. The variations in the value of R C will give consequent variations in the response of the record. Fig. 15 shows two logs with the same logging speed but different ratemeter time constant, which give different shapes of curves. Fig. 16 shows two logs with two time constants and different logging speeds.

Table 2 Relation between thickness, logging speed and time constant versus dynamic distortion (From Czubek, 1978)

$\frac{H}{VRC}$	Δ (%)
1	36.79
2	13.53
3	4.98
4	1.83
5	0.67

2.7.2 The natural gamma ray log

The gamma ray log is a measurement of the natural radioactivity of the rocks penetrated by the borehole. The principal use of this technique is for the stratigraphy correlation and identification of lithology in boreholes.

Gamma rays, which are high energy electromagnetic waves, are emitted in the same way as alpha and beta particles, from radioactive isotopes in the formation. Because of the low penetration of alpha and beta particles only the gamma radiation is practically measureable. The emission of this radiation is mainly due to the presence of potassium (the ^{40}K isotope) and the products of uranium (mainly ^{238}U) and thorium (^{232}Th) decay series (Stefansson and Steingrímsson, 1980).

The gamma ray log is a useful tool for determination of lithology. The response of the log is related to the intensity of radiation of the formations. Although the distribution of potassium, uranium and thorium is not well known in non-sedimentary rocks, these elements follow the degree of differentiation of the rocks and general patterns can be used. A proposal has been made about the relationship between the SiO_2 contents and the gamma ray intensity in Icelandic rocks (Stefansson and Emmerman, 1980). Fig. 17 shows the relation between SiO_2 content and the gamma ray intensity and the correlation

$$[\gamma] = 3.65\ [SiO_2] - 144 \qquad (18)$$

where:

$[\gamma]$ = API gamma ray units

$[SiO_2]$ = per cent.

In this way it is found to have a correlation coefficient of 0.7 . The results obtained from the natural radiation of gamma rays are found to be useful to distinguish acid units from basic ones. (Sanyal, 1979).

The natural gamma ray log is recorded by a detector which can be a Geiger-Muller or Scintillation Counter (Stefansson and Steingrímsson, 1980). The logging equipment used for the measurements in this report has a Geiger-Muller counter which consists of a cylindrical chamber

being filled with gas of low pressure and containing a central wire at high voltage. When a gamma ray enters the detector it ionizes an electron from the gas. This electron gains high kinetic energy in the high electrical field and can cause another ionization on the way to the central electrode. This process causes ionization by collision and raises a detectable pulse at the terminal of the counter. (Pirson, 1963)

The standardized unit of measuring natural gamma radiation is the API gamma ray unit. This is defined as 5% of difference between the counting rate of high and low radioactive zones in the test pit at the University of Texas in Houston. Two hundred API gamma ray units are the counts registered by the radiation emitted by a special concrete at the University of Texas, containing approximately 24 ppm of Th. 12 ppm of U and 4% K (U and Th is in radioactive equilibrium) (Czubek , 1978). For practical purpose an external source is used for calibration. Before putting the sensor into the hole the source is placed at a certain distance from the probe, and the 120 API gamma ray units level is registered. The natural radioactivity present in the atmosphere (background) must be corrected for in order to know the counting rate that corresponds to the API gamma ray unit.

When the natural gamma ray log is run, the response recorded is the dynamic anomaly, which is different from the static one. Equation (15) shows that the areas under the curves are equal. However, in the gamma ray log we can write a new expression:

$$S = H\, I_{\infty} \qquad (19)$$

(Czubek , 1978)

where H = thickness of the radioactive layer

I_{∞} = Intensity of radiation when $H \to \infty$

In this case the intensity recorded is supposed to be the same as the static anomaly. Therefore this is a function of the statistical variations, and the variance in the recorded value of J(Z, V, RC) becomes:

$$\tau^2 [J(Z, V, RC)] = \frac{1}{2RC}\, J\left(Z, V, \frac{RC}{2}\right) \qquad (20)$$

(Czubek , 1978)

If $I(z)$ remains constant, for $T >> 0$, the function $J(Z,V,\frac{RC}{2})$ is equal to $I_{(z)}$, and constant, then:

$$\tau^2 (J) = \frac{1}{2RCJ} = \frac{1}{2RCI} \qquad (21)$$

(Czubek , 1978)

For a given anomaly, we have that.

$$\tau^2 [J(Z,V,RC)] = \frac{1}{ZRC} \times \begin{cases} 0 & Z \leq 0 \\ I\,[1-\exp(-\frac{2Z}{VRC})] & 0 \leq Z \leq H \\ I\,[1-\exp(-\frac{2H}{VRC})]\exp(-2\frac{Z-H}{VRC}) & Z \geq H \end{cases}$$

when $Z = H$, we have from (21)

$$\tau^2 (J\ max) = \frac{1}{2RC} \cdot I\,[1 - \exp(-\frac{2H}{VRC})] \qquad (22)$$

(Czubek , 1978)

or the relative standard deviation:

$$\frac{\tau\ (J\ max)}{J\ max)} = \frac{1}{\sqrt{2RCI}} \sqrt{\frac{1+\Delta}{1-\Delta}} \qquad (23)$$

(Czubek , 1978)

If we record the statistical variation at a defined depth, waiting long enough to have the factor $\sqrt{\frac{1+\Delta}{1-\Delta}}$ equal to 1 , the variations observed should be in the limit of $\pm\ \tau$. By this method we are able to calculate the error in the recorded intensity which will be:

$$I - \tau \leq I_{True} \leq I + \tau \qquad (24)$$

(Czubek , 1978)

The intensity of the radiation is given by the amount of radioactive material present in the rock per unit of weight q (Czubek , 1978). If we assume an infinite homogeneous medium, with the specific radioactivity of q , the counting rate I_∞ , will be:

$$I_\infty = K\,q \qquad (25)$$

(Czubek , 1978)

where K is a factor of proportionality.
This equation is valid in an infinite homogeneous medium and when this medium is traversed by a dry hole. When the drillhole is filled with water or drilling fluid, the recorded intensity is influenced by several variables such as the radius of the borehole (R), radius of the probe (R_s), density of the fluid (ρ), effective mass absorption coefficient for the drilling fluid ($\mu\rho$, taken as 0.03 ρ for the natural radioactivity of the rocks) and the position of the tool in the borehole (ε) (Czubek, 1978). Assuming the tool to be entirely decentralized in the well the log is corrected by a factor C F which is related to the parameters mentioned above. The value of true intensity is:

$$I_\infty = CF \cdot I \qquad (26)$$

(Czubek , 1978)

The value of the borehole absorption function $A\rho$ ($\mu\rho$) is related to the C F by the relation:

$$C\ F = \frac{1}{1 - A\rho\ (\mu\rho R)} \qquad (27)$$

(Czubek , 1978)

and is given in Fig. 18 for the case of the probe being completely decentralized, which is the most common case.

The final considerations of the influence on the natural gamma ray log are for semi infinite homogeneous medium. The intensity depends on these changes and the behaviour of the gamma ray curve in the vicinity of the boundaries of the semi infinite layer is:

$$F(z) = \frac{I(z)}{I_\infty} \cdot C\ F \qquad (28)$$

(Czubek , 1978)

and is represented in Fig. (19) where we can see that the half value of the anomaly occurs at the boundary of the radioactive layer.

In practical measurements the response obtained is influenced by the radius of the borehole and the length of the detector. Fig. 20 and and Fig. 21 show the shape of the curve influenced by the radius of the borehole and the length of the probe, where the shape of the anomaly $F_L(z)$, influenced by the length L of the detector is given by:

$$F_L(z) = \frac{1}{L} \int_{2-\frac{L}{2}}^{2+\frac{L}{2}} F_o(z)\, dz \qquad (29)$$

(Czubek , 1978)

where $F_{o(z)}$ is the anomaly when L = O.

As said before, the thickness of the layer influences the value recorded and consequently the shape of the curve obtained. Fig. 22 illustrates this shape for 3 layers of different thicknesses.

The layer H_3 has a thickness very much larger than the range of investigation. Thus a flat maximum equal to I_∞ with the half value of the maximum at the boundary of the radioactive layer is obtained. The layer H_2 is of less thickness, same as the range of investigation, and has a response with a value of I . No flat region is registrated but a real value equal to I_∞ is found and always with the half maximum at the boundaries of the radioactive layer. H_1 has a thickness less than the radius of investigation. The maximum value is less than the real value, and consequently the half of the maximum value is not at the boundaries, indicating a layer of larger thickness than it is.

When a log is to be interpreted all these possibilities have to be taken into account.

2.7.3 The neutron-neutron log

The neutron-neutron log is sensitive to the porosity of the formations traversed by the borehole. As other nuclear logs, it can be recorded in cased or uncased wells. A neutron source and a detector are placed into the borehole. The detector measures the scattering of the neutrons in the geological formations.

Neutrons are electrically neutral particles and together with the protons form the nucleus of the atom. They have a mass which is almost identical to the mass of the nucleus of hydrogen. When a neutron source is placed in a borehole, high energy neutrons are emitted from the source. These fast neutrons collide with nuclei of the material in the formations, loosing some energy in each collision. The fast neutrons collide with different kinds of nuclei, but the heaviest ones, do not slow the neutrons

significantly. Higher slow down is acheived when they collide with nuclei of approximately the equal mass. The hydrogen nucleus, being of the same mass as neutrons, causes a major energy transfer per collision in the formations. When the neutron is slowed down by successive collisions to lower levels of energy, the thermal state is reached at last. After the neutron has reached the thermal equilibrium with the environment it is finally absorbed. The neutrons can be absorbed by the surrounding nucleus. This absorption excites the nucleus and causes an emission of gamma radiation.

The neutron-neutron log is performed using a probe placed into the borehole, with a fixed distance between the source and the detector. The neutrons are slowed down in the formation and a detector for thermal neutrons registers the intensity of the neutrons. The source used is an Americium-Berillium source. Normally the log is run together with the natural gamma ray log.

The calibration of neutron-neutron logs is usually made in API neutron units, which are related to the difference between two formations of different porosity. The API neutron unit is defined as 1/1000 of the tools response to 19% porosity Indiana limestone, at a test pit situated at the University of Texas in Houston.

The data recorded depends on the volume of material being investigated. This depends on the minimum thickness of the layer that can be investigated, which is equal to the spacing between the source and the detector (Czubek, 1978). However, the record is influenced in some manner by the borehole diameter, mud density, and casing effects, if the log is recorded in a cased well.

2.7.4 The gamma-gamma logs

Gamma-gamma logs are used to measure the bulk density of the formations in the borehole. This log records the intensity of the scattered gamma radiation by the formations. Similar to the neutron-neutron log, the spacing between the source and the detector determines the minimum thickness of the layer to be investigated (Czubek , 1978).

The gamma-gamma log is recorded in such a way that photons absorbed and scattered in the formation are registered. The degradation of gamma rays occurs mainly in three processes (Dresser-Atlas, 1974):

1) Compton scattering: this effect takes place when a photon looses a part of its energy to an orbital electron. This process is observed with gamma rays with energies within 0.1 to 1 Mev and the cross section is proportional to the number of electrons. The response is affected by the number of photons detected by the probe.

2) Photo electric effect. Similar as above, a photon is sent from the source, but when it collides with an electron it looses completely its energy, ejecting electrons from the atom. The detector registers only gamma rays. This process occurs with low energy photons, 0.1 Mev or less.

3) Pair production: This effect takes account of the equivalence of mass and energy proposed by Einstein ($E = m c^2$). This occurs when the photon approaches the nucleus and produces an electron pair. One positron and one negatron, having each an energy of 0.51 Mev. Hence, the energy required by the photon is at least 1.02 Mev.

These three effects are represented in fig. 23, 24 and 25 respectively.

Of all of these processes, the Compton effect is the principal one for what takes place for gamma-gamma scattering. Since the gamma radiation absorbed in the Compton effect is proportional to the number of electrons, and the electron density is proportional to the bulk density of the material being logged, the counts registered can be related directly to the bulk density of the formations.

The logs recorded are from tools where both source and detector are located. A source of 125 M Cu, ^{137}Cs, and a Geiger Muller detector have been used in this study. The distance between the source and the detector was approximately 55 cm. The response is recorded by the detector, and sent to electronic equipment at the surface in the same way as in the record of natural gamma rays.

The calibration of the tools is made by using special pits with different densities. These pits consist of concrete with different concentrations of iron pulver (Jonsson and Stefansson 1980). Their density (as given

in Table 2) was determined by the ratio between their volume and their weight. Three different pits with holes cased with 7.6 cm diameter plastic pipe of 3 mm thickness are used. The effect of the pipe is assumed to be negligible and the calibration is assumed to be valid for open hole.

Table 3

Weight, volume and density for each of the calibration pits used in the calibration of gamma-gamma tools (From Jonsson and Stefansson, 1980)

Pit No.	Weight (kg)	Vol (cm^3)	Density (kg/cm^3)
1	180.45	52988	3.41 ± 0.06
2	130.60	51238	2.70 ± 0.06
3	126.24	51150	2.47 ± 0.06

Jonsson and Stefansson (1980) used a logarithic relationship between the counting rate of the gamma-gamma and the density.

Since the gamma-gamma measurements are related to the counts of gamma rays scattered by the medium and are affected along the way between the formations and the detector, the changes in borehole conditions must be calculated for detailed studies. The factors that can affect the response are water level, changes in the fluid filling the borehole and the diameter of the well. If the log is run in a cased well, the effect of casing and collars must be taken into account. Jonsson and Stefansson (1980) found that the casing causes an offset in the counting rate and in its sensibility. Fig. 26 shows the differences between two logs run in the same well cased and uncased.

3 INTERPRETATION OF GEOPHYSICAL LOGGING DATA FROM THE SVARTSENGI FIELD

3.1 Introduction

Eleven geophysical parameters have been measured in well SG-9. Fig. 29 shows ten of these parameters. Detailed interpretation of all of these is not possible in this short report, due to the relatively short time available for this work. Detailed interpretation needs the knowledge of the work that has been done previously in the field, and a good knowledge of the principles of the logs and their behaviour when the logs are disturbed by extraneous effects. This is the author's first attempt to do this kind of studies and all the requirements for a detailed work are not satisfied. However, a general interpretation of the results is made in a qualitative form and the main effects caused by external parameters are discussed.

Five of the eleven measured parameters are used in this study, but the other parameters are mentioned when their results are relevant for the discussion of the interpretation. The large variations found in the diameter of the well, make it difficult to obtain high accuracy in the interpretation. The size of the well influences the results obtained in the logs, mainly the nuclear ones. In general a good correlation is found with the geological interpretation already made for the area. The results are discussed in general for each of the logs, and four sections of the well are taken for detailed studies of the correlation between the different types of logs recorded. Three of these sections are chosen on basis of the geology, but one for purely geophysical reasons.

3.2 The caliper log

The caliper is used to obtain the variations in the average diameter along the well. Strong changes are found, from the top to 595 m depth. These changes follow the rate of penetration in the drilling process and are mainly related to soft formations, fractured zones and in some cases to aquifers.

The drill bits used for drilling the hole were 17 1/2" diameter to 585 m depth, and 12 1/2" diameter from 585 m to the bottom at 994 m. It is normal to expect a difference in the diameter of the hole, but

the size observed in this hole is beyond expectations. Cavities up to 28 inches where found, mainly in the first 600 m. Comparison with the differential temperature shows that at shallow depths, where the diameter of the well changes greatly, the temperature rises, but not in the sections where relatively minor changes occur. It is thought that these changes in temperature are related to aquifers. Comparison of this data with other observations at the same depths supports this statement.

3.3 The natural gamma ray log

Despite the problems connected with the determination of the correction factor due to the variations in the diameter of the well, the results of the measurements fit fairly well with the lithology of the well obtained from petrographical analyses of the drill cuttings. The counting rate is almost constant along the borehole, and the variations can be attributed more to the irregularity of the diameter in the well and statistical variations than to different chemical composition of the rocks. Due to the strong changes in the size of the well, which affect the counting rate, it is difficult to see clearly the boundaries between different layers. By taking the almost constant counting rate, it is assumed that all the formations are similar in chemical composition. Exceptions are the anomalies found at 530 m depth and at 865 m depth. The latter anomaly is not taken for discussion due to problems explained later.

Several points along the borehole were taken for the calculations of the true natural gamma ray intensity. Each point with its respective value of diameter, where the gamma curve shows the same behaviour. It is found that the highest intensity corresponds to the concentration of SiO_2 of 51% and the lowest value corresponds to 46%. An average of all of these points gives the value of 48.9% of SiO_2 . This value is in good agreement with the values reported by Jakobsson et al. (1978) of 28 surface samples of lavas collected in the area, where the average of all the samples shows the content of SiO_2 of 48.23%. This result of the natural gamma ray, permits us to state that the formations traversed by the hole SG-9 are mainly composed of basaltic lavas, which is in agreement with evidence and experience gained in other wells and by surface exploration. Although the values recorded, where the shape of

the gamma ray curve present no drastic variations, fit well with the expected geology, anomalous values of the gamma ray intensity are found from 530 m to 539 m depth. If this anomaly is due to different SiO_2 content, this is an abnormally high content of SiO_2 for the characteristic basaltic nature of the area. The anomaly starts at 530 m, and values for each meter of depth were taken in this section as well as in the 10 m above and below the zone. The SiO_2 values calculated from the gamma anomalies give the results of basaltic formations with 48% of SiO_2 above the anomaly and 48.6% of SiO_2 below. In the section between 530-539 m the average value of 51.9% of SiO_2 was found. The maximum and minimum values found in the units are 54.3% and 51.3% respectively. It is possible that these anomalous values are a tool effect, however, the different geophysical methods, run with different equipment and at different time in this well, show an anomaly at the same depth. Therefore the explanation of an error in the instrument is not very convincing. The SiO_2 value of 52% does not deviate significantly from the usual content of SiO_2 in basalt. It is therefore proposed that the layer between 530 m to 539 m depth has slightly higher silica concentration than other parts of the well.

The second anomalous values are found at 865 m depth and are of the order of 180 API gamma ray units, which is much higher than the former values. Though the response of the tool seems to be a true response, problems with the electronics started at 600 m during the logging. It can therefore not be excluded that this anomaly is due to malfunction in the instrumentation.

Unfortunately only one measurement was run at this depth, and it is not possible to claim for its validity. However, if the log is run again later and the same anomaly is found, the statement of the presence of acidic units in the Reykjanes peninsula could be claimed. This would be the first occurrence of acid or intermediate rocks in the Reykjanes peninsula. The value of 180 API gamma ray units corresponds to SiO_2 concentration greater than 80%.

3.4 The neutron-neutron log

The high permeability of the Svartsengi geothermal field is well known (Kjaran et al. 1979). The porosity determinations carried out by the

neutron-neutron log show high porosity values. The problem of correction of the values due to the diameter of the well consisted of both the fact that no correction curve for the diameter of the well is available and because of the strong changes in this diameter in short intervals. The first problem was solved by calculating a correction curve for the average of the diameter of the well used. The curve calculated is valid for 18" diameter of the well. This curve was constructed by taking the values in Stefansson (1979) and extrapolating the diameter for different porosities. By using these values, which relate the intensities and diameters, and extrapolating the curves to 18", the resulting curve has more or less the same shape as the others. Its accuracy is not as good as the others, but relative values that are of our interest can be obtained. The second problem was more difficult to solve, because a new curve had to be constructed for each diameter of the well. For the calculations, points were taken from sections where the minimum variations are present in the caliper log. Fig. 27 shows the curve used for calibration of the porosity together with the reference curves.

The profile of the neutron-neutron log shows the high porosity of the area. Zones of low porosity were found to have 2% porosity and the highest values calculated were about 38%. Layers with the lowest porosity values are found within the depth range 70 m and 300 m. There several relatively thin layers, 20 m or less, are intercalated by high porosity formations. Below 300 m depth the porosity is more constant, but a few low porosity layers are found. The neutron-neutron porosity values obtained are in good agreement with the values obtained from the 16" and 64" resistivity logs and the gamma-gamma log. Also a good correlation is found with the soft formations where the cavities are detected by the caliper log, and with the differential temperature log. The high porosity zones correspond to strong changes shown by the other logs.

3.5 The gamma-gamma log

In principle, the results of the natural gamma ray show that the rock layers present in the well, are of similar chemical composition. This makes it reasonable to expect the values of the matrix density of these formations to be similar. In the same way as in the neutron-neutron logs, problems were found with the calibration curves for the diameter of the

well. A curve was adapted from Jonsson and Stefansson (1980). Assuming the most dense part of the well to have the density of 3.0×10^3 kg/m^3 the count rate of 120 c.p.s. was obtained for this density. The variation in counting rate was assumed the same as in Jonsson and Stefansson (1980). The values of density were found in the interval $(2.5\text{-}3.0) \cdot 10^3$ kg/m^3. Fig. 28 shows the curve used for the calibration together with the curve of reference that was made for the 7.5 cm diameter test pit.

3.6 The resistivity logs

The two normal resistivity logs 16" and 64" were run. The curves in both logs have the same tendencies. The 64" log shows in general higher resistivity values. The highest values are related to zones of high density and low porosity, and inversely the lowest resistivity values with low density and high porosity and the main cavities along the borehole. Due to the extremely irregular diameter of the well, the lower values are not taken for correlation. The values taken for analyses are from portions where the well does not present a great amount of cavities or where the cavities are not so big. Despite the limitation in choosing the values for the study, the correlations with other parameters is found good. Even where the results are affected by the variations in diameter of the hole.

3.7 The self-potential log

The interpretation of self-potential is difficult in volcanic rocks. As a first attempt a qualitative interpretation can be made in intervals where the permeability is enough to produce natural potential by the migration of ions from formations with higher salinity to these with lower concentrations. The changes in the potential detected in the log run in well SG-9 have a good fit with the values shown by the porosity and density logs, and even with the changes in the differential temperature. The anomaly in the natural gamma ray log at 530 m depth shows a negative potential with respect to the reference point at the surface. This suggests a stream potential, caused by an inflow at this depth.

3.8 The temperature and differential temperature logs

Temperature profiles were run in the hole recording the maximum temperature of 235°C at the bottom of the hole. The reservoir is assumed to be a convection system. The differential temperature run in the cooled well shows a good correlation with aquifers and in some cases with cavities and resistivity anomalies. Also the two main production zones at 565 m depth and 900 m depth show up as changes in the differential temperature log. It is proposed that the increment in the values of the differential temperature, related with cavities, high porosities and low resistivities are in some cases due to aquifers present in the hole.

3.9 The cement bond log

The cement bond log was run in the well in order to investigate the cementing job. This log shows zones where the cement is rather bonded, but in general the cementation of the well is far from being good. The log shows higher attenuation of the wave where the diameter has the less drastical changes. The higher the peaks the larger the cavities and looser the bond of the cement.

3.10 Correlation between different logs

Four sections of the well were taken for these correlations. The first one from 140-170 m depth, was chosen because in this section of the well, the diameter had the most regular form in the upper part of the well, and the normal resistivity log showed a high resistivity with a relatively low porosity. The second section is a 100 m section where the different curves present much changes. Not all values are used for the correlation, but only the values where there are relatively small changes in the diameter. The third section was selected to present an increase in the intensity of neutron-neutron and a location where a big cavity is detected by the caliper log. The fourth section is chosen due to its anomalous count rate in the natural gamma ray log.

Section at 140-170 m. An almost normal diameter of the well is found over this depth interval, presenting only strong changes from 140 to 147 m, and a small cavity of about 18" at 152 m, with the rest of approximately 17 1/2", which is the size of the drill bit used. The natural gamma ray shows the normal values for basaltic formations, having an average of 50% of SiO_2. The values of porosity range from 13% at 155 m to 35% at 162 m depth. Lower counting rates of about 411 API neutrons units were measured but that data was not used because it is out of the range of the calibration curve, and is caused by the effect of the big cavities where these values were found. The same effect of cavities was found in the results of the short normal resistivity log in the upper and lower part being of the order of 3 Ωm, but not in the long normal, where the lowest value was of 6 Ωm at 170 m depth, but other values ranging from 8 to 64 Ωm. The 8 Ωm value is found in the small cavities and the 64 Ωm value at 157 m depth, where the well presents the best performance. The results of gamma-gamma shows an almost equal density in the section, with the values within $(2.75 - 2.80) \times 10^3$ kg/m^3. These results indicate that the highest values of SiO_2 could be due to some changes in the basaltic formation. The results obtained in self potential and differential temperature show a good correlation with the other logs. At 157.5 m depth a negative self potential appears and coincides with a rise in the temperature. The resistivity decreases, the porosity increases and the caliper shows a series of cavities at this depth. These results can be interpreted as due to the presence of aquifers at this depth.

Section at 260-370 m. The natural gamma radiation indicates homogeneity of composition of the rocks at this depth. The lowest counting rate is of 16 API gamma ray units, where the well has the diameter of 18.5". The correction factor calculated for this diameter is 1.54 . The intensity corrected to 26.6 API gamma units, corresponds to 47% of SiO_2 content. The higher value in the interval is 24.8 API gamma ray units, for a diameter of 17.8" . The correction factor of 1.49 is found and the intensity of 36.9 API gamma units corresponds to a SiO_2 content of 50%. The average value of SiO_2 in the interval is 48.8%. The values obtained from the neutron-neutron log are from 373 API neutron units to 1012 API neutron units. There are a few values that are not possible to take for calculating the porosity, being between 373 to 530 API neutron units. The lowest porosity observed was of 5% corresponding to 1000 API neutron units, and the maximum value of 38% porosity corresponds to the values of

approximately 550 API neutron units. The gamma-gamma log shows the values of density between $(2.5 - 2.9) \times 10^3$ kg/m^3. Though the diameter of the well is far from being regular, the values of resistivity do not look affected by this irregularity. The values of the short normal resistivity are within reasonable limits, having values of 12 Ωm as the maximum and 2.0 Ωm as the minimum. The long normal resistivity seems to show the real resistivity values of the formation, having the maximum value of 40 Ωm and the minimum of 5 Ωm. An exception is the value of 2 Ωm where the same value was found using the short normal probe. The self potential shows a negative gradient but not as strong as found in the other sections. It can however be interpretated as being caused by a streaming potential, like in the section at 140-170 m depth. There is a correlation of the S.P. curve with the differential temperature. Four major increments of temperature, related with the other results, are interpretated as aquifers.

Section at 450-470 m depth. This section was chosen not because of the regularity of the diameter of the well, but for the changes in counting rates observed, mainly in the neutron-neutron log. The diameter is far from regular going from 19" to 23.5", and with strong changes, over intervals of half a meter. The corrections of the intensities are not good enough. This is especially the case for the porosity determination. The values selected were from places where the well presents almost the same diameter. Hence it has not been possible to make any meaningful cross plots. However, the absence of cuttings from this depth makes it desirable to try at least a relative correlation in this section. The natural gamma ray log shows a rather high count rate for the normal basaltic formation. Values of 52% SiO_2 are found, but the limits of error are large because of the strong change in diameter. The average value is found to be 50% of SiO_2 which is near the limits of basaltic formations. The porosity is high, and higher than in other layers. It was only possible to determine three values of porosity, because the others were too low for the calibration curve. The three values obtained are 20% at 455 m depth, 16% at 458 m, and 26% at the bottom of the anomaly at 460 m depth. The value of 16% could be less, due to the fact that it is near a cavity and could be affected by water contained in it. The density appears to be rather constant, and shows values among the lowest registered in the well. The density is found to be between 2.5×10^3 and 2.6×10^3 kg/m^3. The short normal resistivity log shows low values

of resistivity between 2 Ωm and 2.6 Ωm and the 64" tool shows values between 2.4 Ωm and 4 Ωm. The self potential increases approximately 15 mV in the interval of 448 to 468 m depth. No strong changes are found in the differential temperature. The extremely low counting rates in the neutron-neutron log (even if account is taken of affects by the diameter of the well), and the non-recovery of cuttings, suggest a high porosity in this zone if not a highly fractured rock. It is possible to see in the changes of the shape of the neutron-neutron curve, together with the caliper log, that it is a zone formed by several thin layers with high porosity between them. This could be the cause of the low counting rate in the neutron-neutron response. The high values of SiO_2 together with the almost constant low resistivity values suggest that the formation is tuff or breccia.

Section at 530-539 m depth. This section, as was mentioned in the gamma ray discussion, was the only one that shows a really different shape in the gamma ray curve. These values of gamma ray intensity are not characteristic for basaltic formations but for andesitic ones. The neutron-neutron gives the result of an extremely porous formation, almost all the points give more than 40% of porosity in the curve. For this reason they are not plotted. The values of gamma-gamma give rather high values of density along the borehole with values from $(2.90 - 2.95) \times 10^3$ kg/m^3. The resistivity values are from 0.8 Ωm to 2 Ωm in the short normal arrangement and from 1 Ωm to 2.2 Ωm in the long normal. The S.P. curve shows a drastic negative gradient at this depth, but no great changes occur in differential temperature. All these parameters, which are shown in Table 4, suggest that this layer may be of a somewhat different composition than the other geological units in the well.

The relatively high density, the high porosity, the low resistivity, even affected by external parameters, and the negative gradient in the S.P. curve, suggest that there is a distinguishible geological formation between 530 and 539 m depth.

The geophysical logs do, however, not reveal what is the most appropriate description of this formation.

Table 4

Values of SiO_2 , porosity, density and resistivity obtained from the logs at the interval 530-539 m.

Depth	SiO_2 (%)	ϕ (%)	ρ (x10^3 kg/m^3)	Ωm(64")
530	49.6	38	2.95	2.2
531	51.3	>40	2.95	1.6
532	51.6	>40	2.95	1.4
533	53.6	>40	2.95	1.4
534	51.3	>40	2.90	1.4
535	51.0	>40	2.90	1.2
536	51.3	>40	2.90	1.4
537	51.3	>40	2.90	1.2
538	54.3	>40	2.90	1.4
539	52.0	>40	2.95	1.0

3.11 Correlation with other studies

Different studies carried out in the Svartsengi area show that the rock formations in the geothermal field are of homogeneous basaltic composition. Surface exploration and borehole geology shows the strata to be composed of lavas and hyaloclastites of basaltic composition. Former geophysical logging is in good agreement with the logging results of well SG-9.

The borhole geology study of well SG-9 (Flores, 1980), carried out at the same time as the borehole geophysics, is in a rather good agreement with the geophysical determinations, except for the natural gamma ray anomaly found at 530 m depth. Unfortunately no cuttings were recovered at this depth for correlation.

The two first sections chosen for detailed geophysical studies, at 140-170 m and 260-370 m , are described as basalts from the studies of the rock cuttings, which is in good agreement with the geophysical determination. No cuttings were recovered in the third section from 450 to 470 m , but a layer of hyaloclastite tuff appears at 498 m depth. The suggestion based on the results of the geophysical logs that the formation is tuff or breccia is found to be likely from a geological point of view.

The many contacts detected in the geological studies were difficult to correlate with the logs, due to the strong changes in the diameter of the well, but generally the correlation was good. A maximum shift of 2 m was found between contacts located from the cuttings and those inferred by the logs (the cuttings are collected at 2 m intervals).

3.12 Conclusions

The results obtained in the geophysical logging in well SG-9 , show that the well is located in a geological environment with rather uniform basaltic compositions. The low resistivity found in the formations is caused mainly by the high porosity of the rocks and the salinity of the geothermal water. The results of the lithology arrived at by the natural gamma ray log are in good agreement with those obtained by geological observations of cuttings recovered from the drilling, except for the high intensity found at 530 m depth. The detailed contacts detected by geological studies of cuttings are difficult to pinpoint exactly from the logs, due to the drastic changes of the diameter of the well.

In spite of the difficulties in the correction and interpretation of the data, the geophysical logs show to be a good tool to detect various parameters characteristic for the rock formations traversed by the drillhole. The correlations between different logs were found good enough to describe the properties of the formations and these are found to be in good agreement with other studies carried out in this well.

ACKNOWLEDGEMENTS

The author is very grateful to the organizers of the 1980 UNU Geothermal Training Programme in Iceland. Special acknowledgement is due to Dr. Valgardur Stefansson for his supervision and the wealth of ideas which he offered the author while preparing this project. The help and advice of Mr. Benedikt Steingrímsson, Mr. Hilmar Sigvaldason and Mr. Gudjon Gudmundsson, during the theoretical and practical work is also recognized. The writer is much indepted to Dr. Ingvar Birgir Fridleifsson for his assistance in Iceland and for critically reviewing the manuscript. Assistance and effort of Gudni Gudmundsson and Sigurdur Hardarson is gratefully acknowledged. Special thanks to Dr. Hjalti Franzson for useful discussions on the geological sequence encountered in the well, to Ms. Sigridur Valdimarsdóttir for typing the manuscript and to Ms. Erna Birna Forberg for drawing the figures. Also many thanks to the lecturers during the introductory course and all the people in ORKUSTOFNUN who helped the author during his stay in Iceland.

REFERENCES

Archie, G.E., 1942: The electrical resistivity log as an aid in determining some reservoir characteristics, Am. Inst. Mining Metall. Engineers Trans., Vol. 146, pp. 54-62.

Arnason, B., 1977: Hydrothermal systems in Iceland traced deuterium, Geothermics, vol. 5, pp. 125-151.

Czubek, J.A., 1978: Lecture series notes at NEA, June 1978 (manuscript).

Dresser Atlas, 1974: Log review I, Dresser Atlas Division, Dresser Industries Inc.

Dresser Atlas, 1980: Catalog - North America.

Flores, J., 1980: Borehole geology of SG-9, Svartsengi geothermal field, SW-Iceland. UNU Geothermal Training Programme, report 1980 - 4.

Gearhart Owen Industries Inc., Catalogue Engineers manual, Vol. 1.

Gearhart Owen Industries Inc., 1975: Formation evaluation data. Handbook, Gearhart-Owen Industries Inc., Forth Worth, Texas, U.S.A.

Gearhart Owen, 1980: Catalog- North America.

Georgsson, L., 1979: Svartsengi, Vidnámsmælingar á utanverdum Reykjanesskaga, Orkustofnun, OS79042/JHD 20.

Jakobsson, S., Jonsson, J., and Shido, F., 1978: Petrology of the western Reykjanes peninsula, Iceland. Journal of Petrology, V. 19,No.4, p.609-705.

Jonsson, J., 1978: Jardfrædikort af Reykjanesskaga, Orkustofnun, OS JHD 7831, April 1978.

Jonsson, G. and Stefansson, V., 1980: Density and porosity logging in IRDP drillhole Reydarfjördur, Iceland, (Manuscript to be published at Journal of Geophysical Research, Special issue).

Keller, G. and Frischknecht, 1966: Electrical methods in geophysical prospecting, Pergamon Press, 517 p.

Keller, G., Murray, J.C. and Towle, G.H., 1974: Geophysical logs from the Kilauea geothermal research drillhole. SPWLA, 15th Annual Logging Symposium, paper L.

Keys, W.S., 1979: Borehole geophysics in igneous and metamorphic rocks. SPWLA, 20th Annual Logging Symposium.

Keys, W.S. and Mac Cary, L.M., 1971: Application of borehole geophysics in water resources investigation. Chapter E-1. Book two in Techniques in water resources investigations, U.S.G.S. Washington, 1971.

Kjaran, S.P., Halldórsson, G.K., Thorhallsson, S. and Elíasson, J., 1979: Reservoir engineering aspects of Svartsengi area, Geothermal Resources Council, Transactions, V. 3, p. 337-39.

Pirson, S.J., 1963: Handbook of well log analysis for oil and gas formation evaluation, Prentice Hall Englewood Cliffs N.J.

Sanyal, S.K., Juprasert, S. and Jusbasche, M., 1979: An evaluation of a rhyolite-basalt volcanic ash science from well logs. SPWLA 20th Annual Logging Symposium, June 3-6, 1979.

Schlumberger, 1972: Log interpretation, Vol.1, Principles.

Stefansson, V. and Emmerman, R., 1980: Gamma ray activity in Icelandic rock (manuscript to appear in JGR, Special issue).

Stefansson, V. and Steingrímsson, B., 1980: Geothermal logging I. An introduction to the technique and interpretation, OS 80017/JHD 09.

Stefansson, V., 1979: Geophysical logging in the IRDP hole in Reydarfjördur Iceland, Report OS 79003/JHD02, National Energy Authority, Reykjavík, 1979.

Thorhallsson, S., 1979: Combined generation of heat and electricity from a geothermal brine at Svartsengi in S.W. Iceland. Geothermal Resources Council, Transactions, Vol. 3, September 1979.

Wyllie, M.R.J., 1963: The fundamentals of well log interpretation: New York, Academic Press, 238 p.

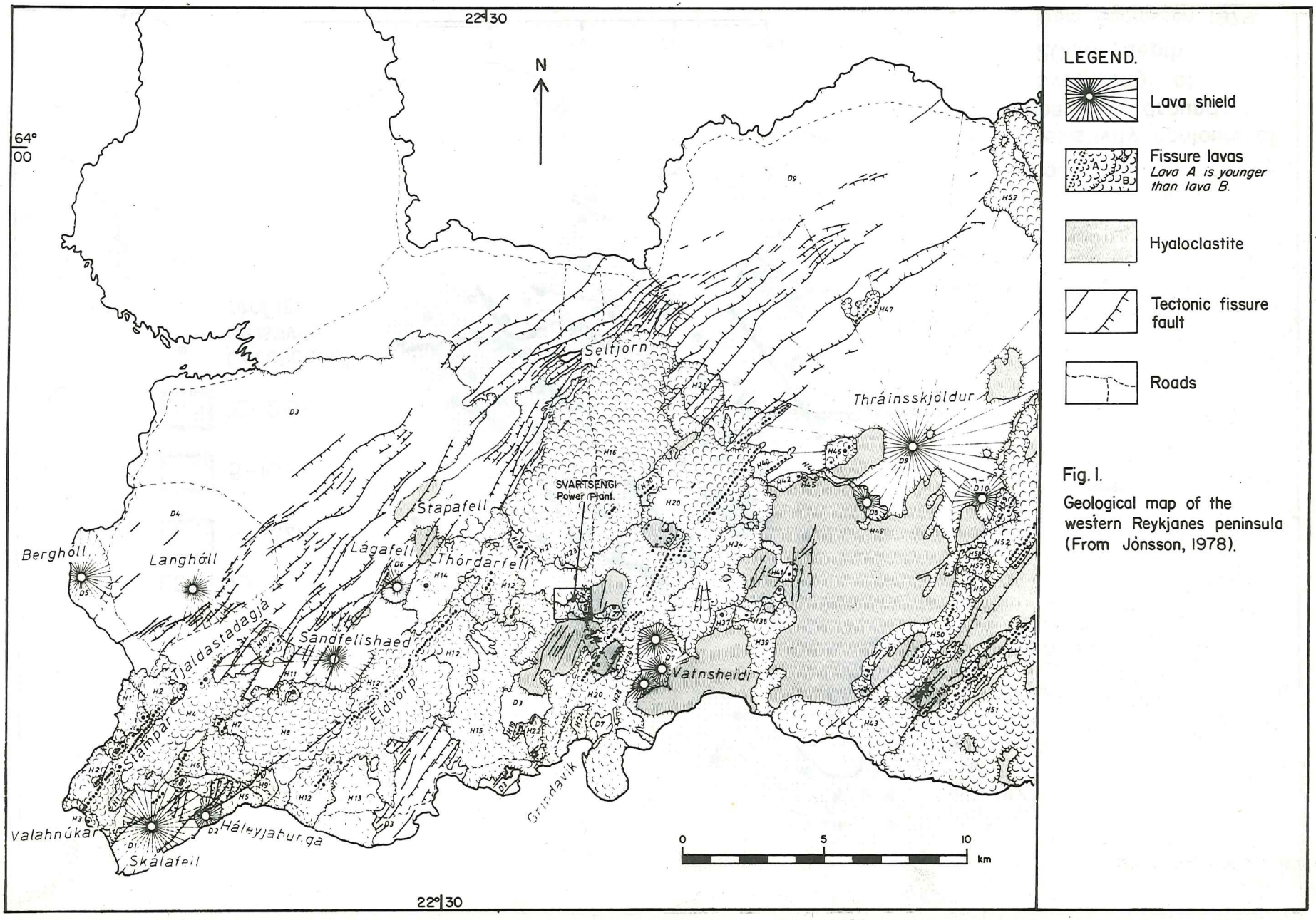

Fig. I.

Geological map of the western Reykjanes peninsula (From Jónsson, 1978).

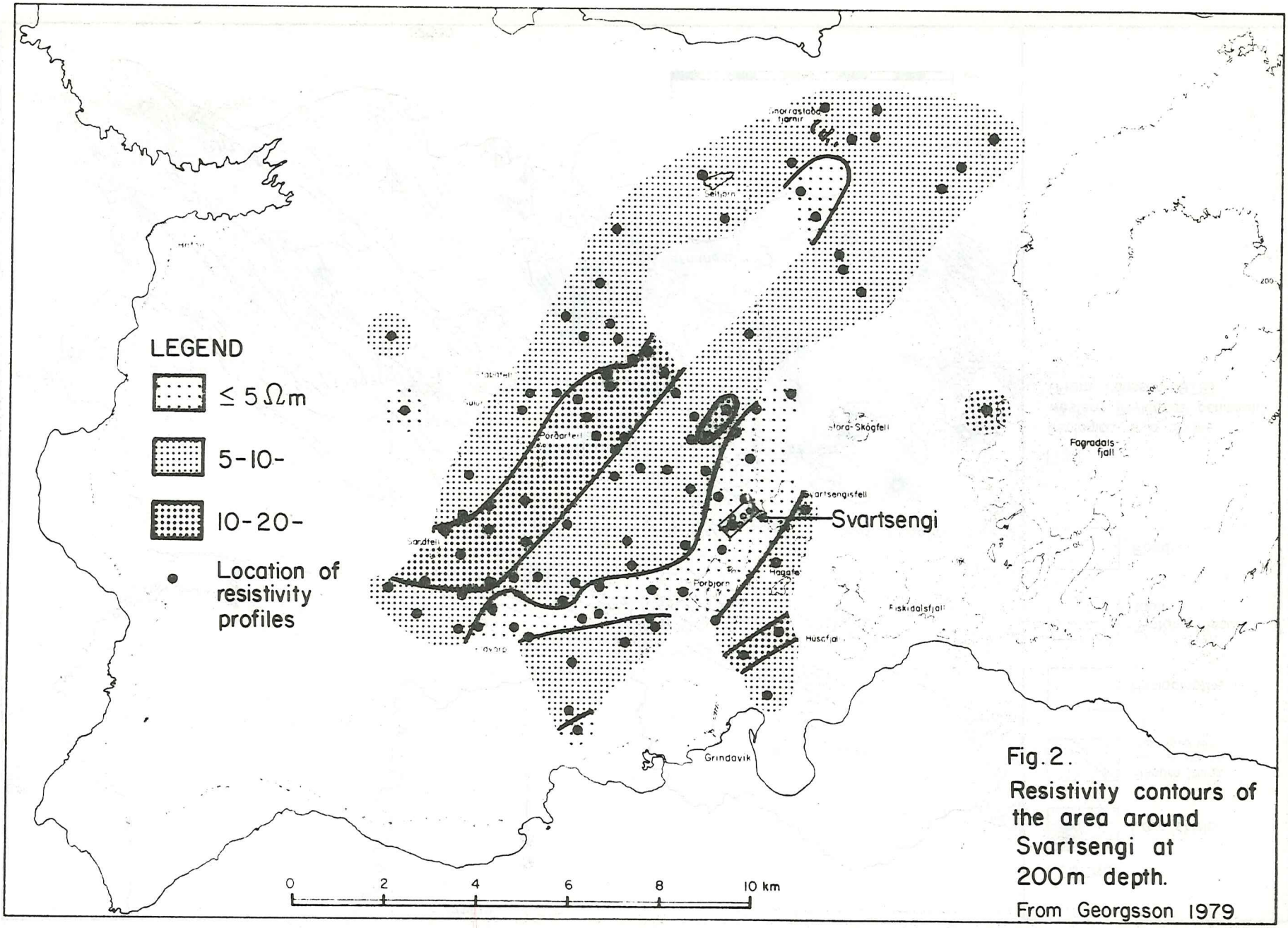

Fig. 2.
Resistivity contours of the area around Svartsengi at 200 m depth.
From Georgsson 1979

F-18362

ORKUSTOFNUN

	'80.10.07.
	Luis/EBF
Three arm caliper probe (Gearhart-Owen industr. 1980)	HSÞ
	F-20076

Fig. 3.

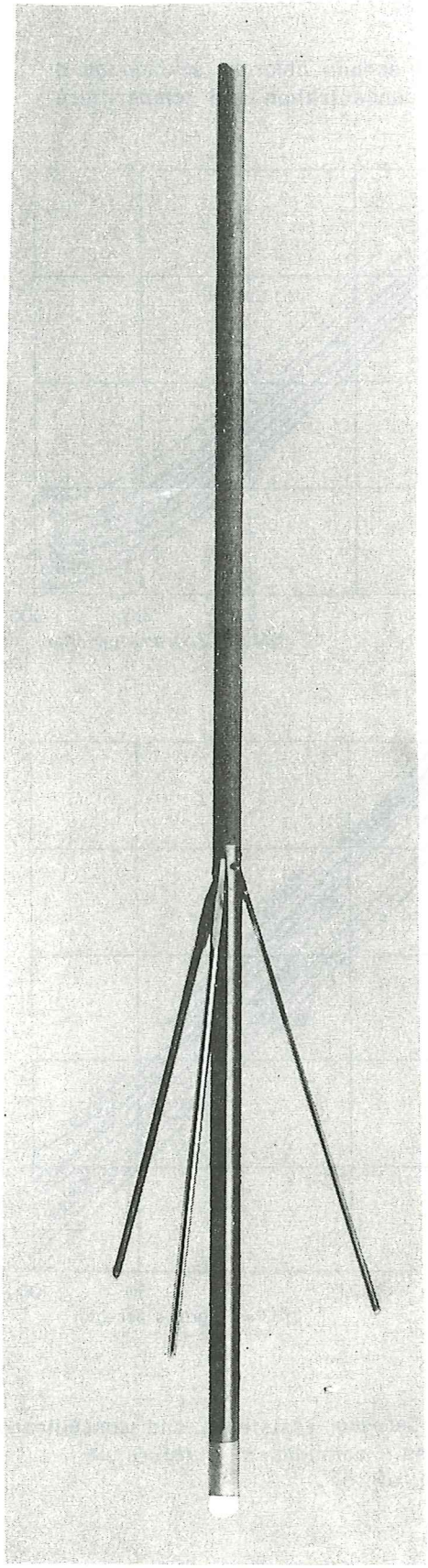

From Gearhart - Owen, 1980.

ORKUSTOFNUN

Relationship between resistivity, and temperature.

'80.09.09
Louis/EBF
HSÞ
F-19995

Fig. 4.

Resistivity of sodium chloride solution as a function of concentration and temperature.

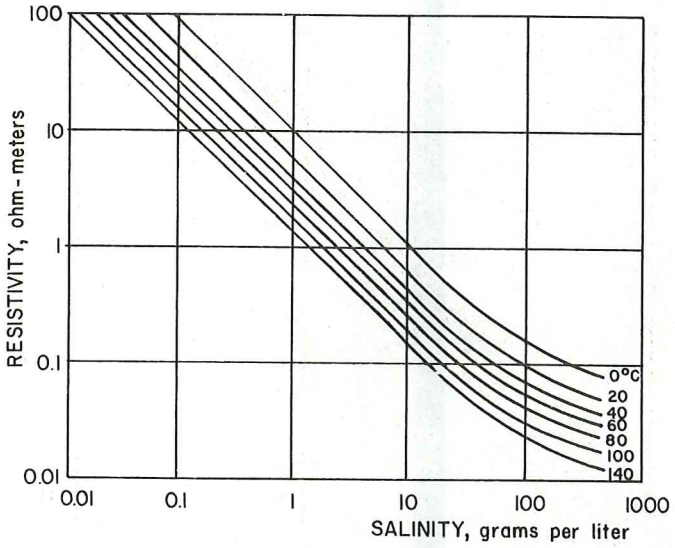

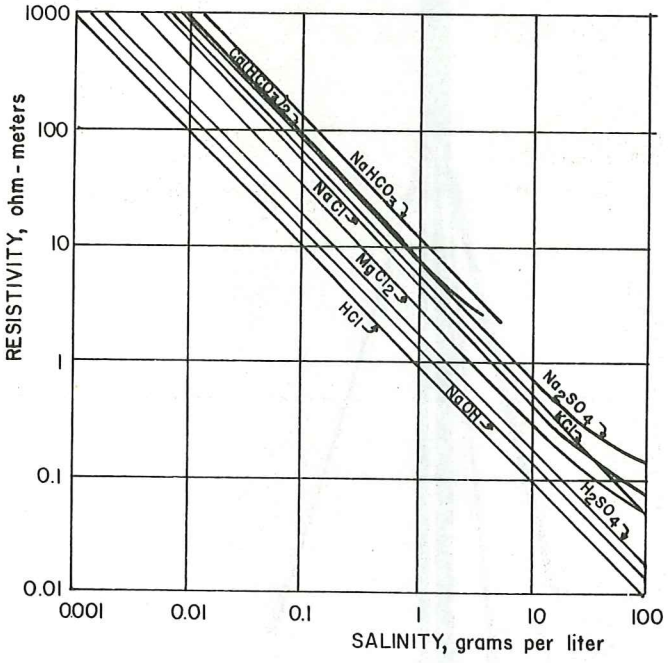

Fig. 5.

Relationship between resistivity and concentration of various salt solutions at a reference temperature of 18°C.

ORKUSTOFNUN

Relationship between aquifer resistivity, porosity and salinity.

'80.09.09
Louis/EBF
HSÞ
F-19997

Fig. 6

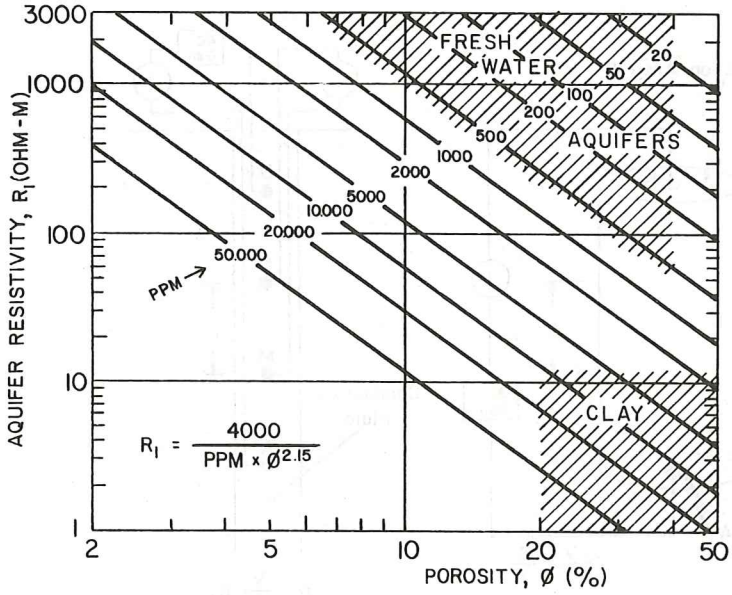

From Keys and MacCary, 1971

ORKUSTOFNUN

Comparison of laboratory resistivity measurements on cores and resistivity logs in boreholes.

'80.09.09.
Louis/EBF
HSÞ
F-19996

Fig. 7.

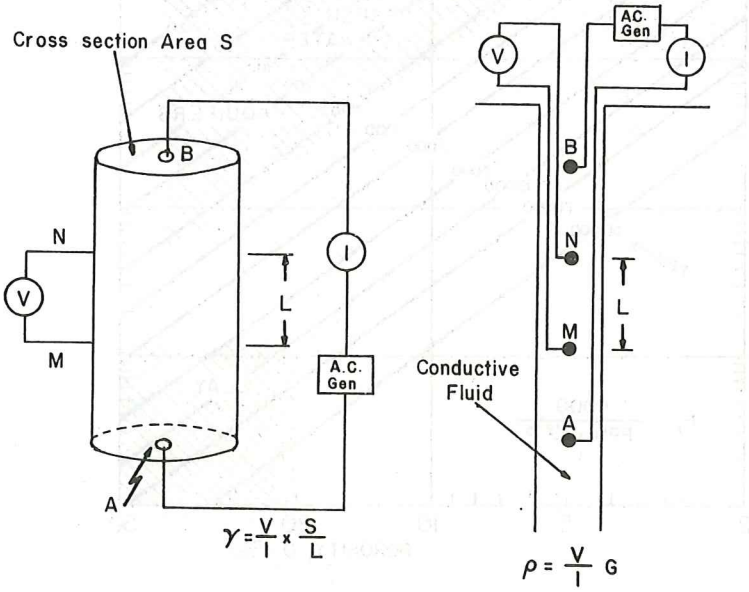

ORKUSTOFNUN

Electrodes arrangement in normal devices.

'80.09.09
Louis/EBF
HSÞ
F-19998

Fig. 8.

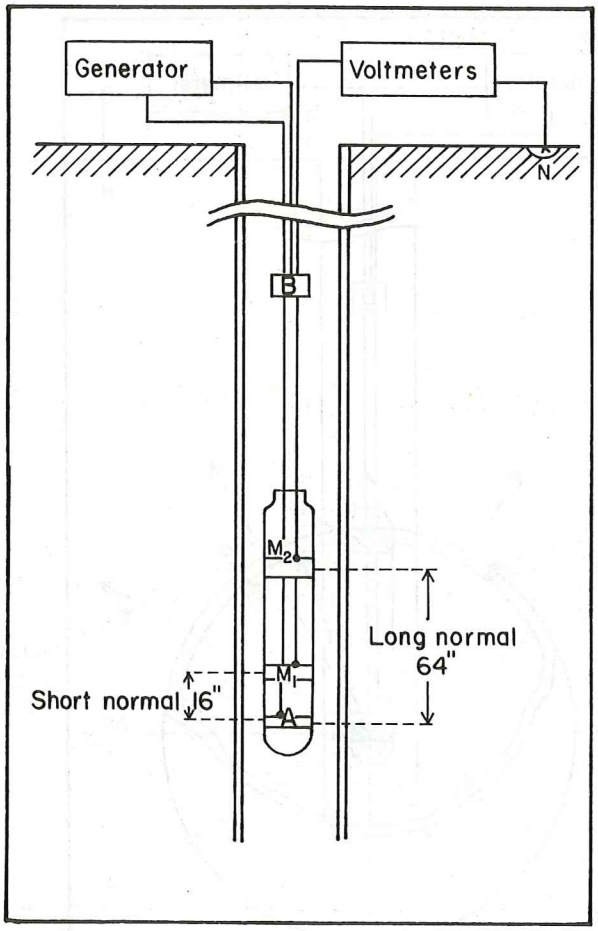

Electrodes arrangement in normal devices.

ORKUSTOFNUN

Determination of the electrical potential by normal devices.

'80.09.09
Louis/EBF
HSÞ
F-19994

Fig. 9.

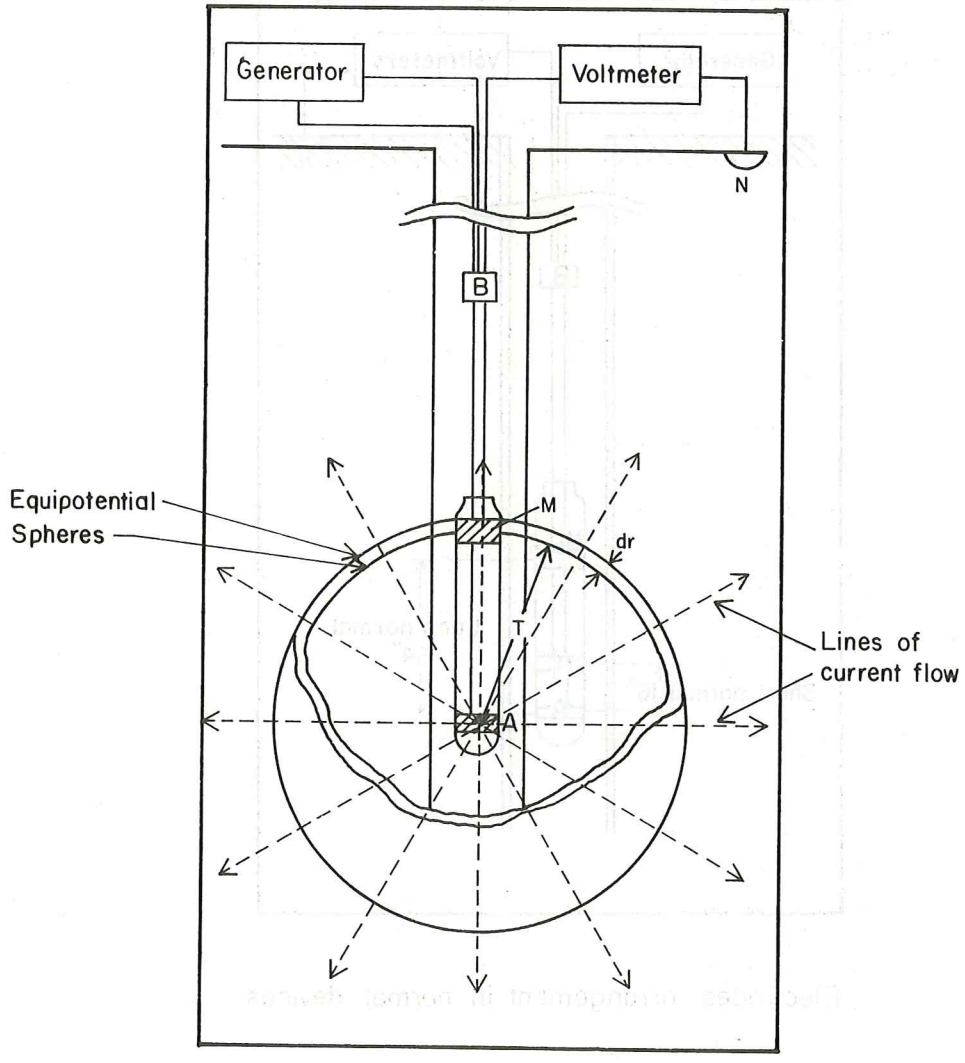

ORKUSTOFNUN

The principles of a natural potential by migration of ions.

'80.09.25.
Luis/EBF
HSÞ
F-20040

Fig.10.

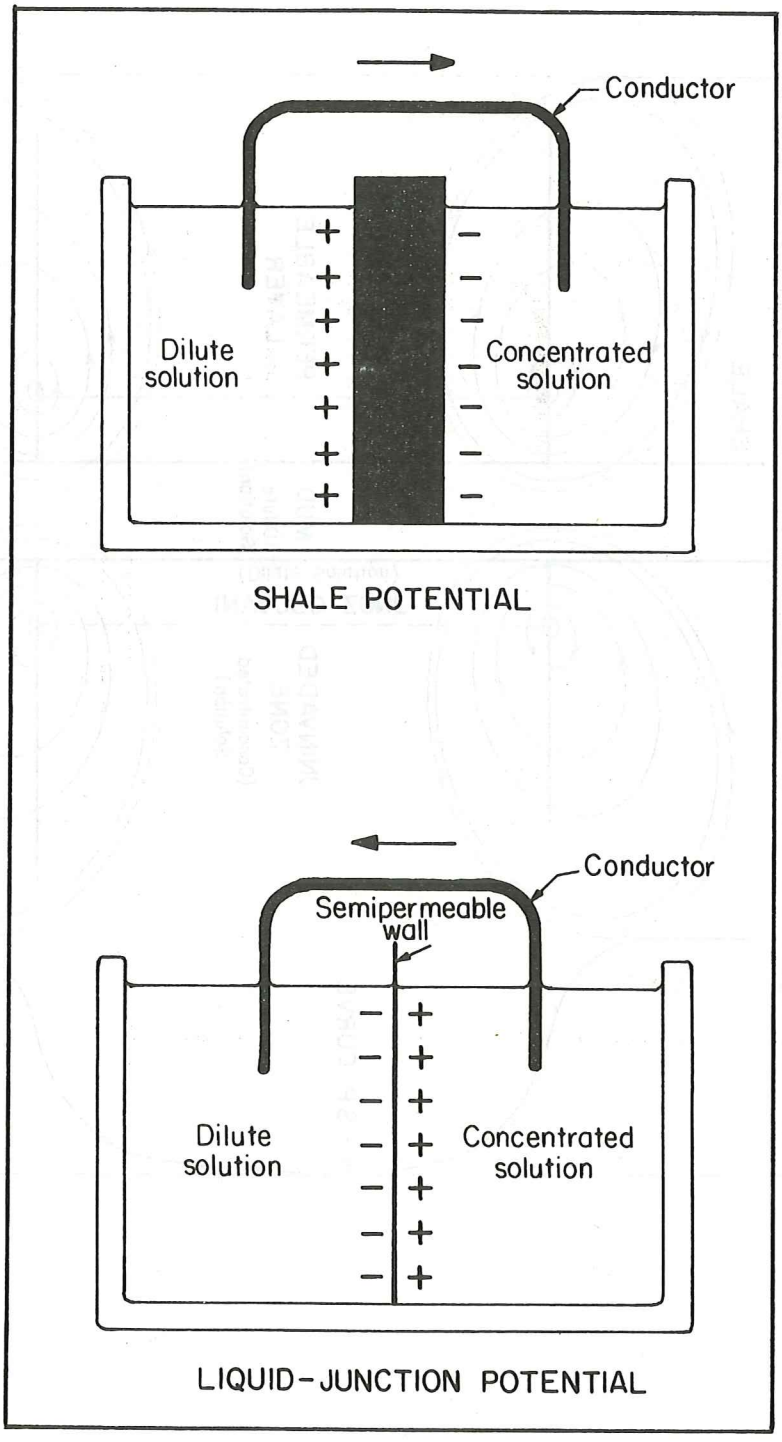

From Dresser Atlas, 1974.

Fig. II.

The S.P. curve and the corresponding electrical field at the boundaries of a permeable layer.

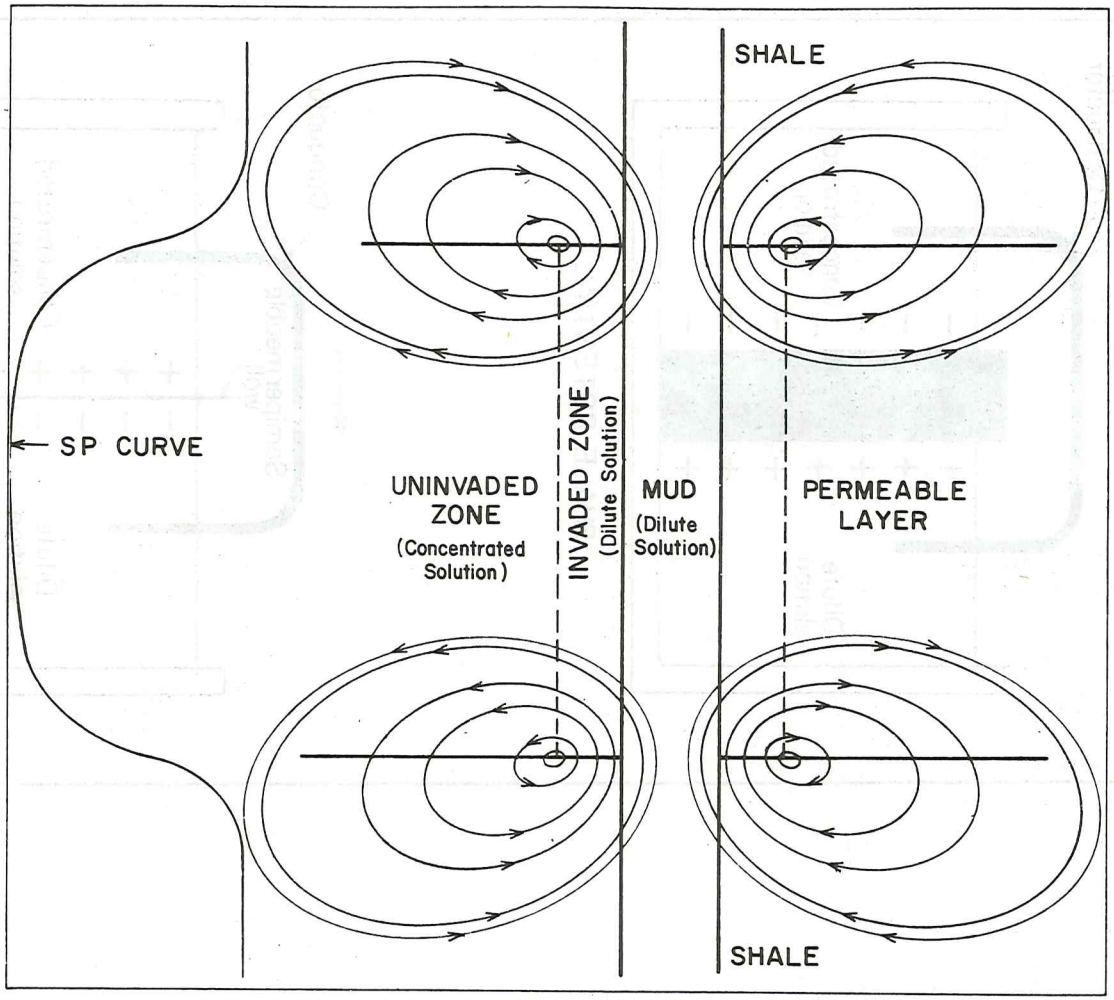

From Dresser Atlas, 1974.

Fig. 12.

S.P. anomalies for three different layer thicknesses, without invasion and 40" invasion.

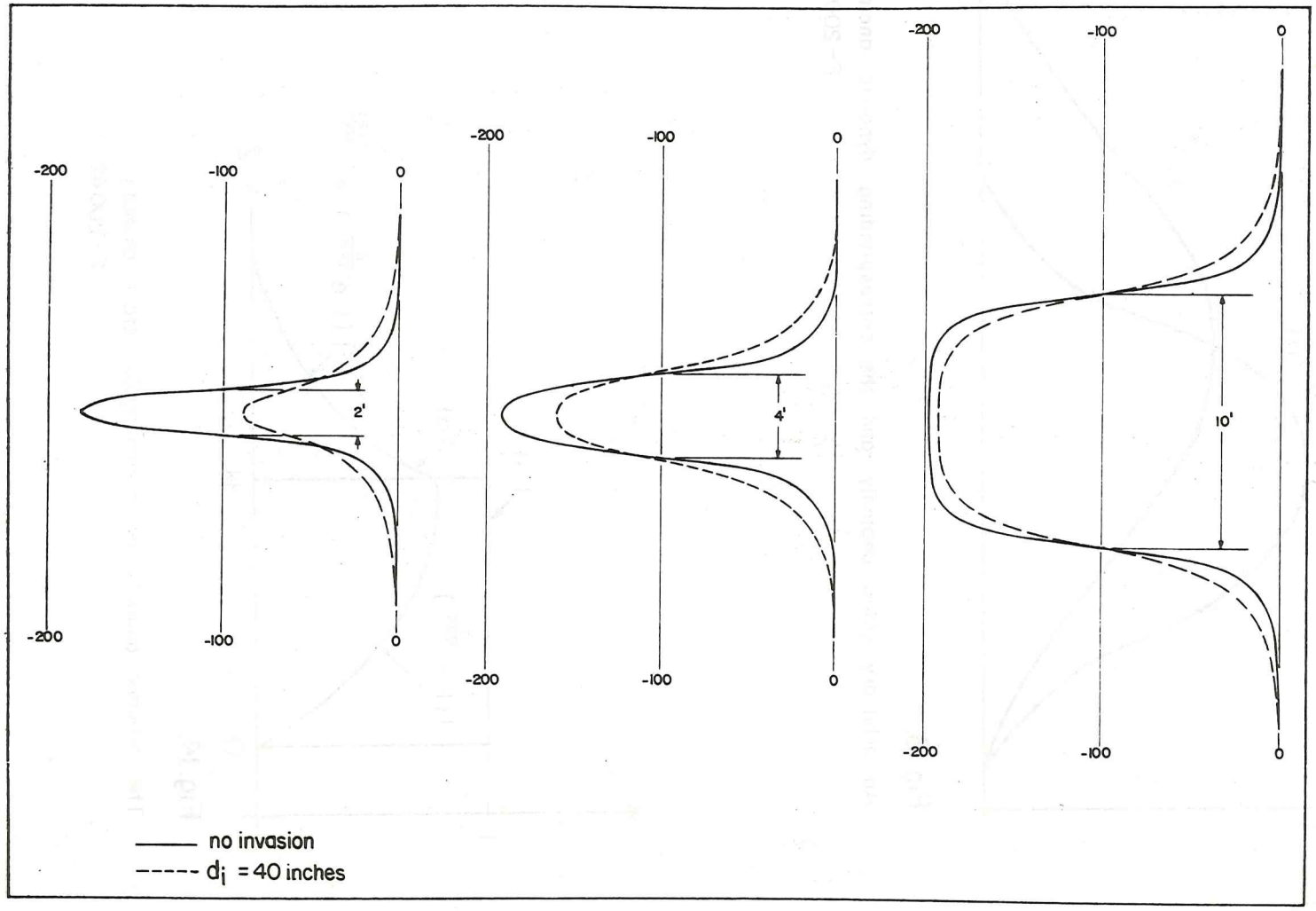

From Dresser Atlas, 1974.

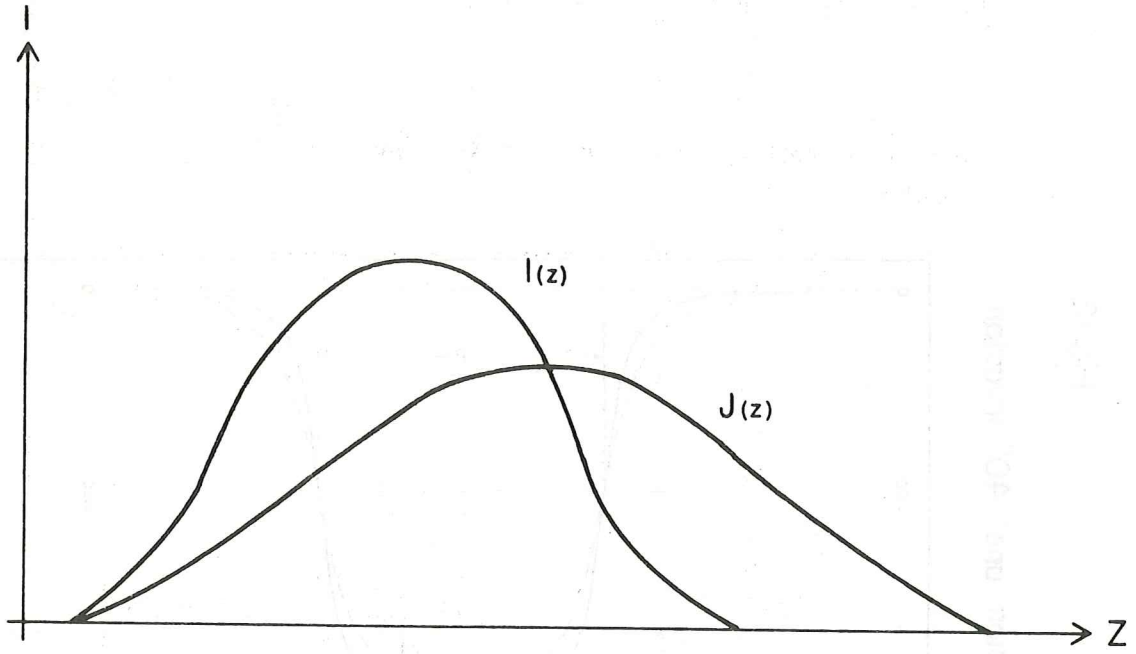

Fig.13.

An arbitrary static anomaly and the corresponding dynamic anomaly.

F-20041.

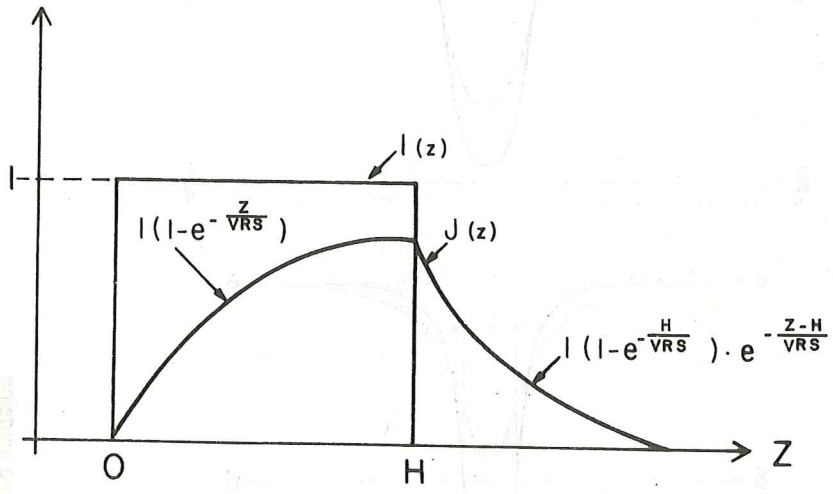

Fig. 14.

The dynamic anomaly for a rectangular static anomaly.

F-20042.

ORKUSTOFNUN

Log response at different time constant and same logging speed.

80.09.05
Luis/EBF
HSP
F-19992

Fig. 15.

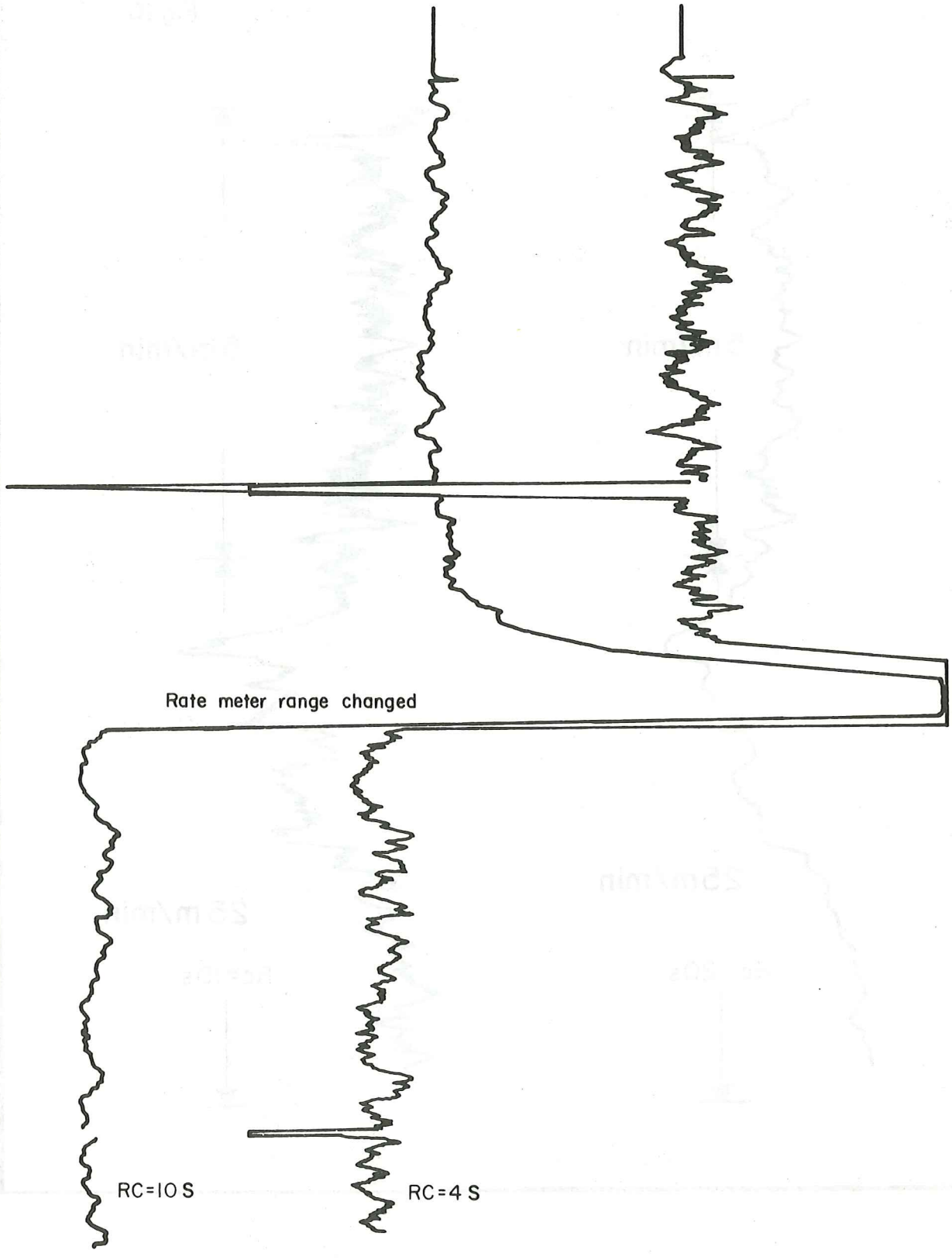

ORKUSTOFNUN

Log response at two different time constants and two different logging speed

80.09.30
Luis/EBF
HSÞ
F-20048

Fig.16

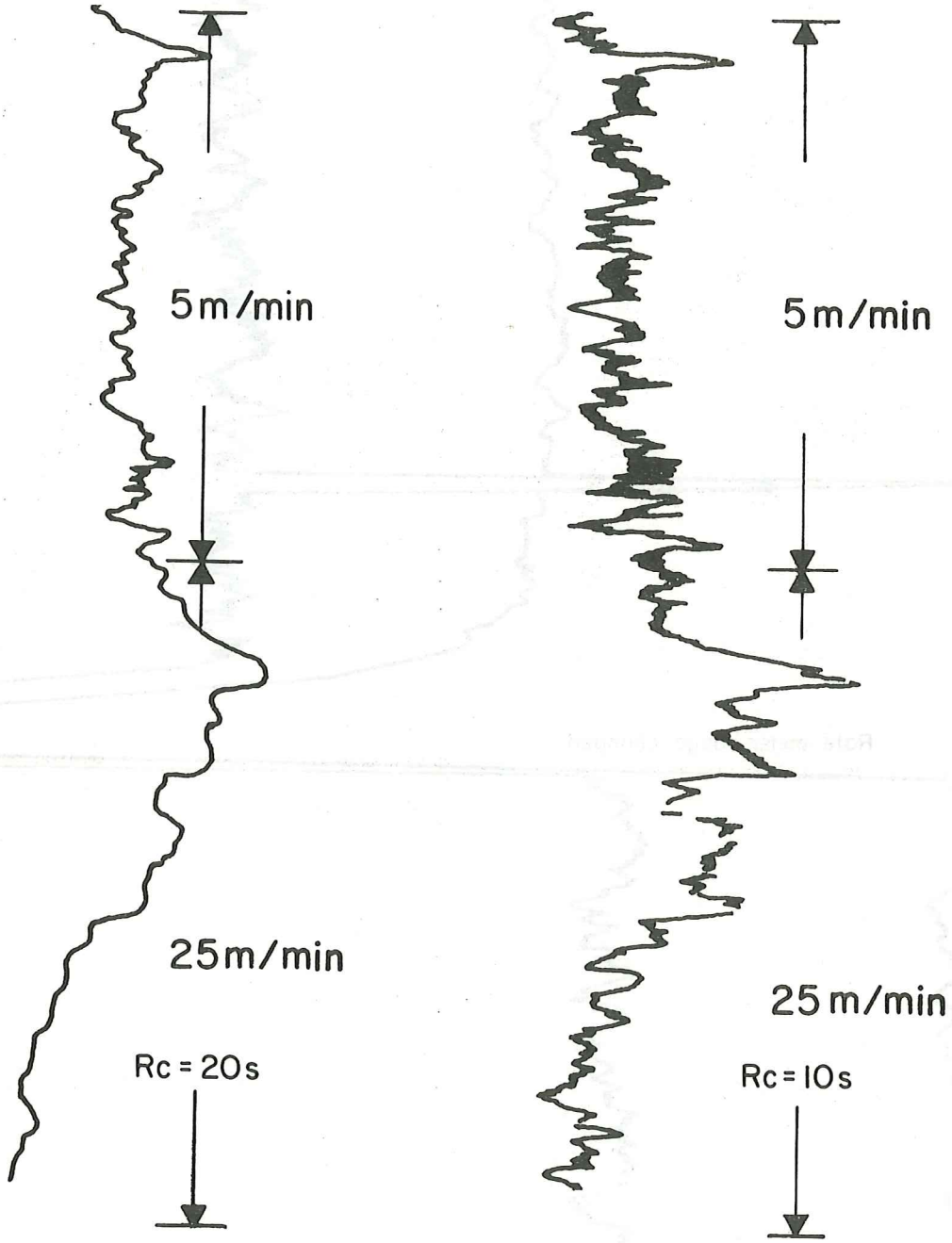

ORKUSTOFNUN

Relation between natural gamma ray intensity and SiO_2 IRDP hole Áreyjar, Reiðarfjörður.

'79.08.10
VS/ab
Múl.
F - 18586

Fig.17.

ORKUSTOFNUN

Absorption function of the borhole fluid.

'80.10.27.
Luis/EBF
HSP.
F- 20148.

Fig. 18.

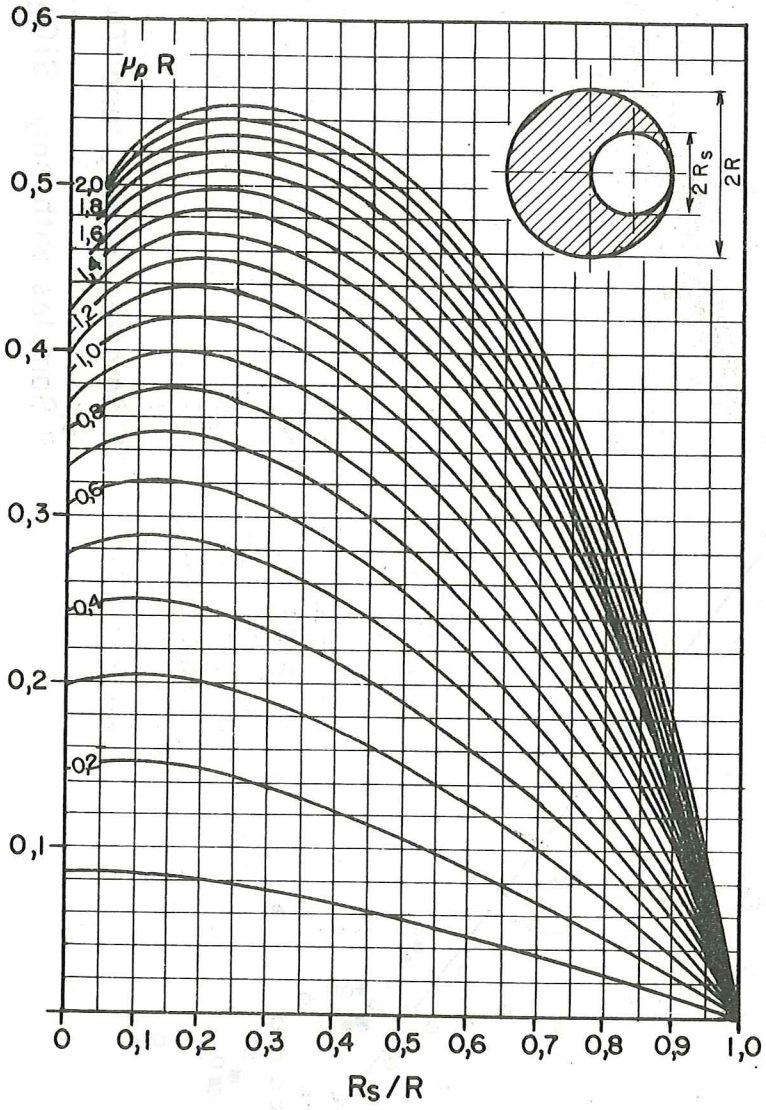

ABSORPTION FUNCTION $A_\rho(\mu_\rho R)$ OF THE BORHOLE FLUID

R -BOREHOLE RADIUS
R_s-PROBE RADIUS
μ_ρ -0,03 · ϱ
ϱ -FLUID DENSITY

From Czubek, 1978

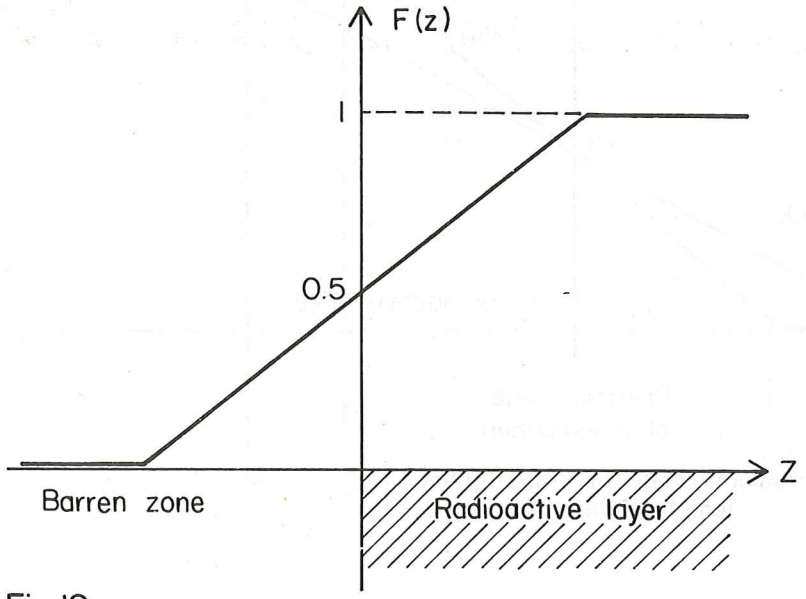

Fig. 19.
Behaviour of the anomaly from a semi infinite radioactive layer.

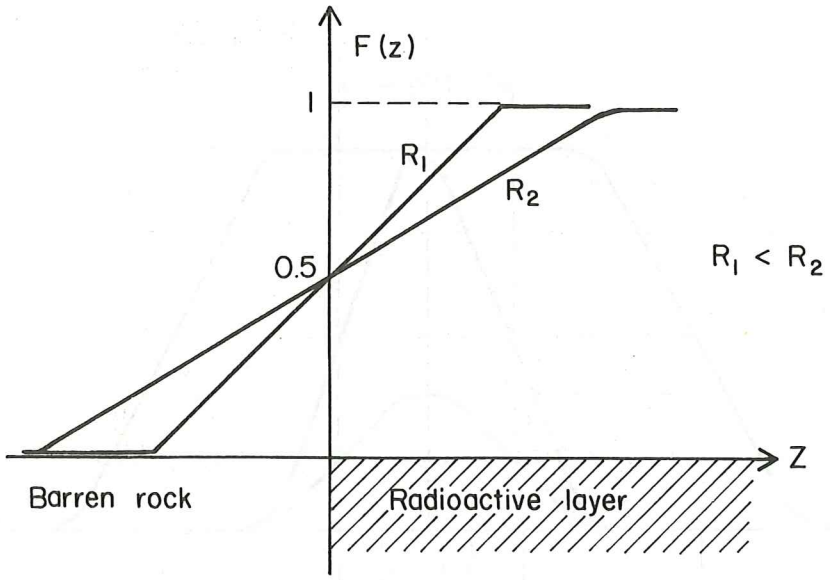

Fig. 20.
Influence of the borhole radius R on the shape of the semi infinite anomaly F(z).

From Czubek, 1978.

F - 20056.

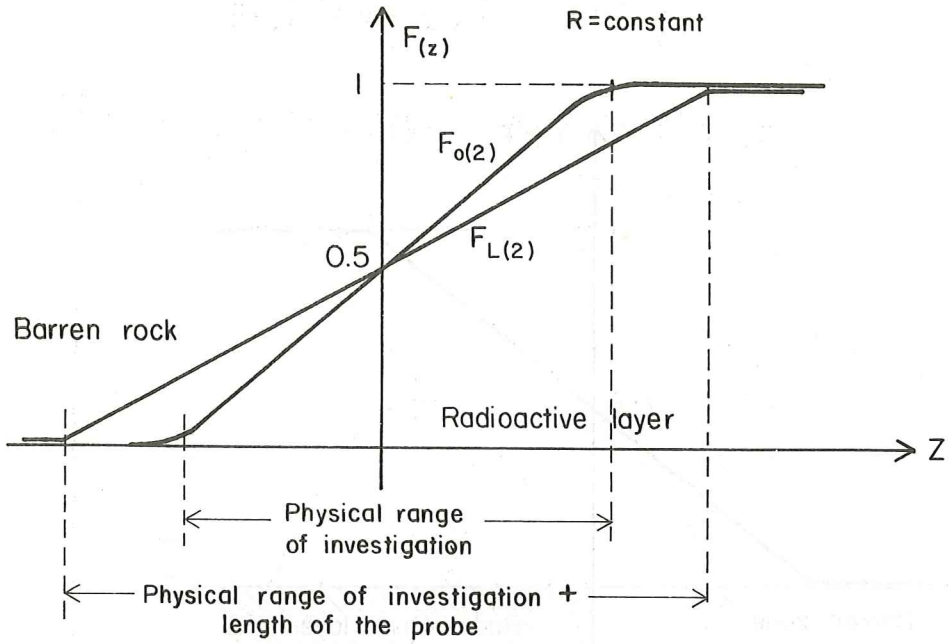

Fig. 21.

Influence of the detector length L on the shape of the semi infinite anomaly.

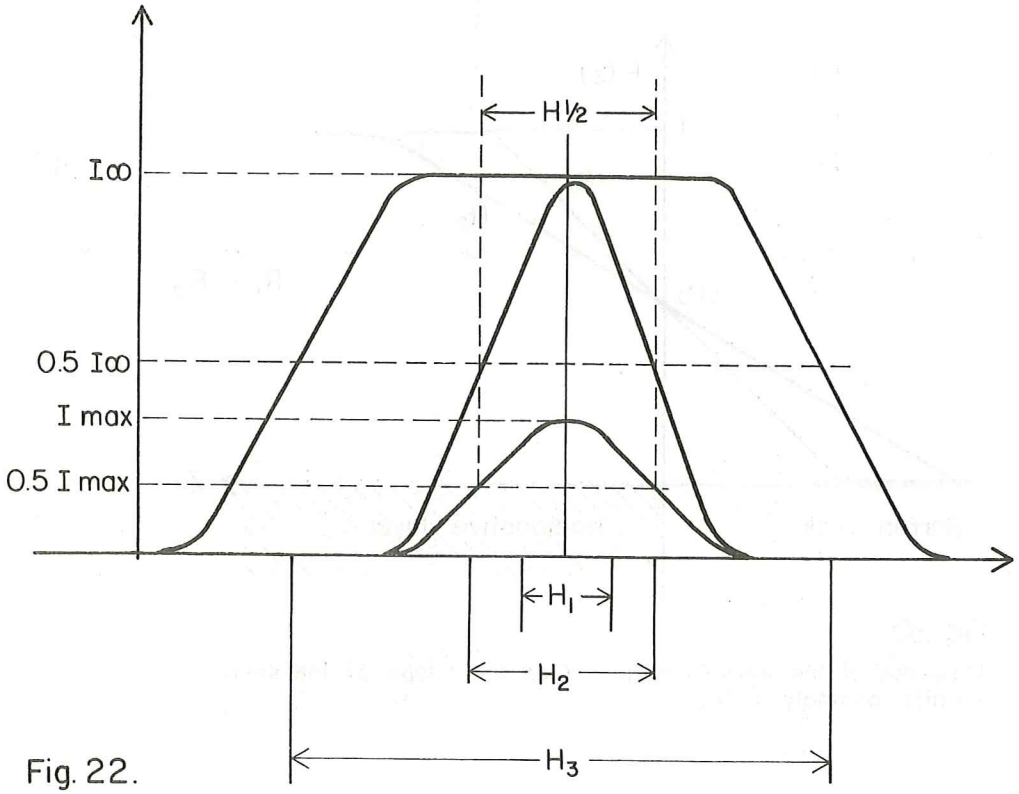

Fig. 22.

Influence of the layer thickness on the shape of radioactive anomaly.

ORKUSTOFNUN	80.10.27.
Degradation of Gamma-rays.	Luis/EBF
	HSÞ
	F-20146.

Fig. 23. **Compton Scattering**

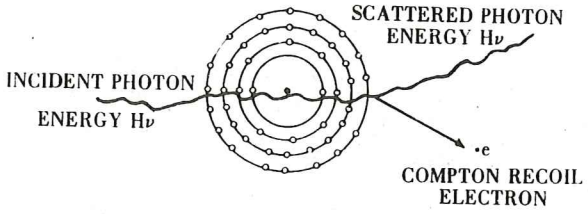

Fig. 24. **Photoelectric Effect**

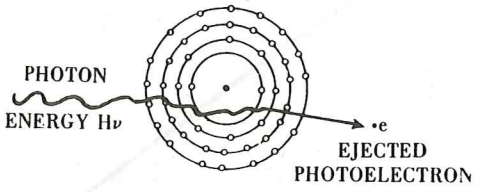

Fig. 25. **Pair Production**

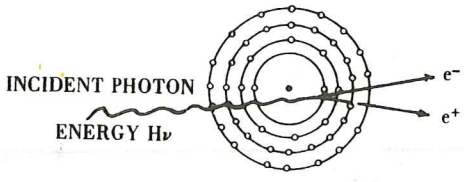

Gamma-gamma response for cased and uncased wells.
(From Jónsson and Stefánsson 1980).

Fig. 26.

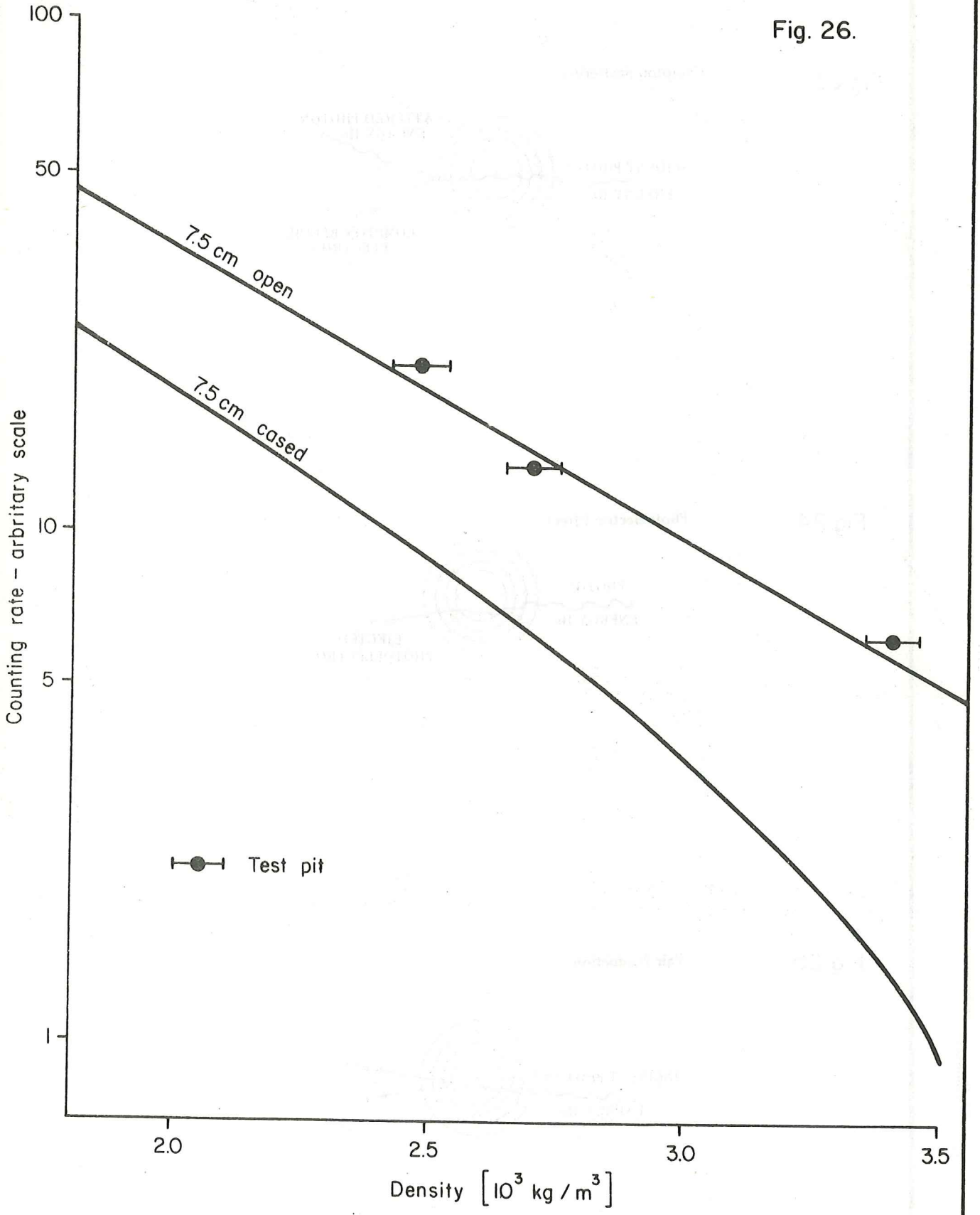

80.05.07., GJ/VS/GSJ, J-Múl., F. 19608

ORKUSTOFNUN

Curve for 18" construeted from the curves valid for 6, 7.5 and 9 inches.

'80.10. 27
Luis/EBF
HSÞ
F-20147.

Fig. 27.

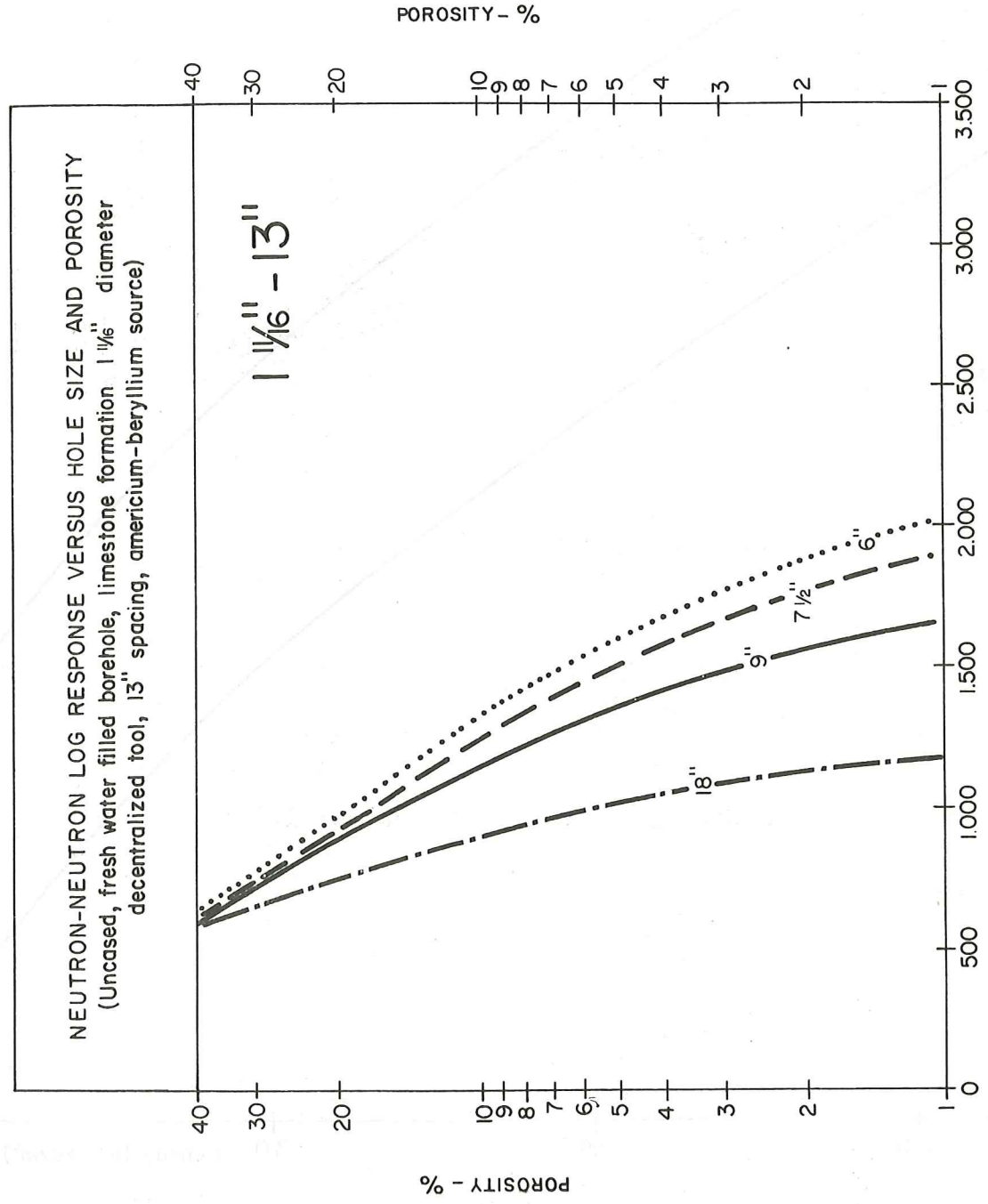

ORKUSTOFNUN

Calibration curves for gamma-gamma log.

'80.10.01.
Luis/EBF
HSÞ. Svartsengi
F-20058.

Fig. 28.

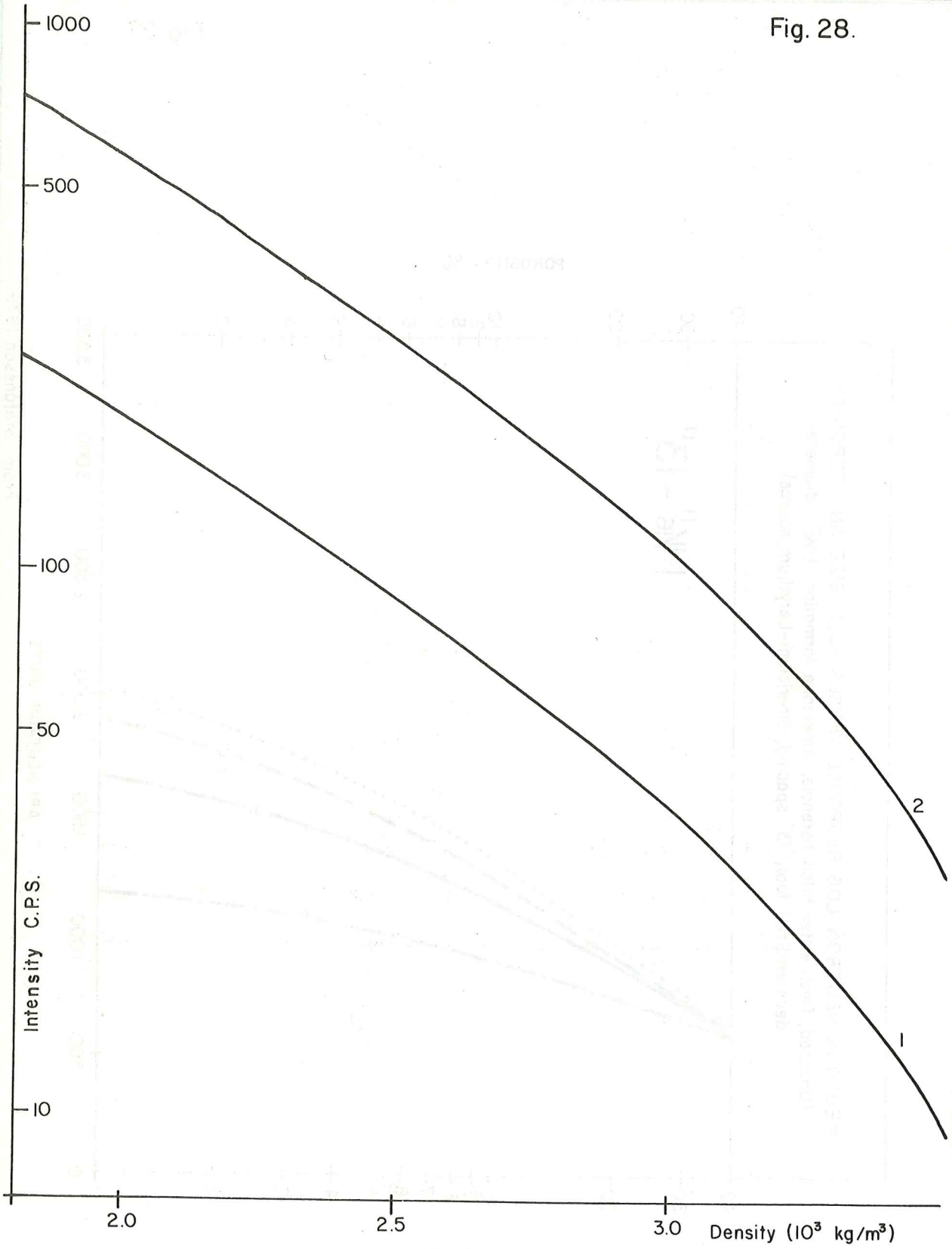

1. Calibration curve for 7.5 cm diameter, cased well (from Jónsson and Stefánsson 1980).

2. Calibration curve 13⅜ inches diameter, cased well (calculated from 1)

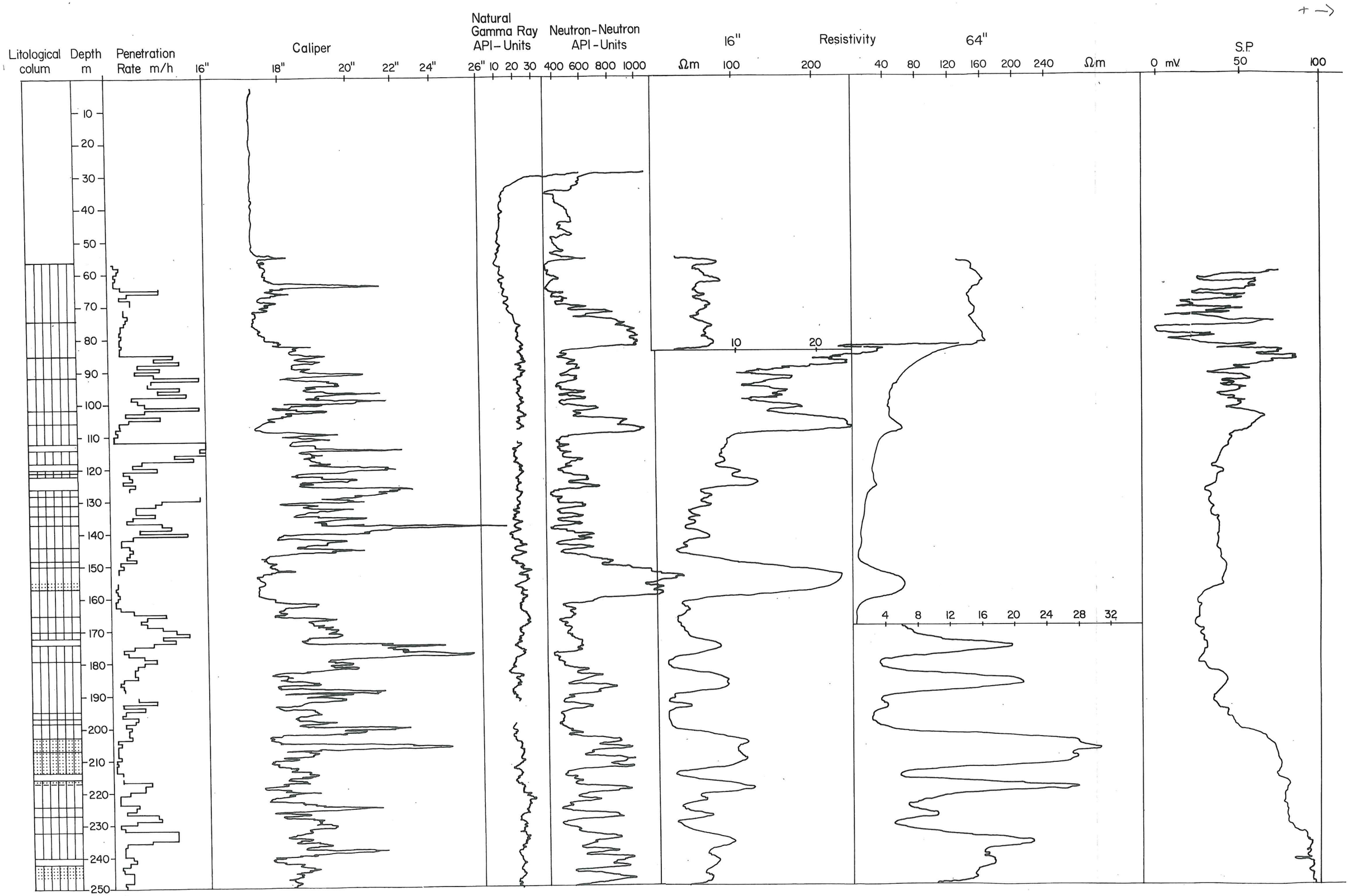
+ →
Litological colum
Depth m
Penetration Rate m/h
16"
Caliper
18"
20"
22"
24"
Natural Gamma Ray API-Units
26" 10 20 30
Neutron-Neutron API-Units
400 600 800 1000
16"
Ωm
100
200
Resistivity
64"
40 80 120 160 200 240
Ωm
0 mV
S.P
50
100
10
20
4 8 12 16 20 24 28 32
10 20 30 40 50 60 70 80 90 100 110 120 130 140 150 160 170 180 190 200 210 220 230 240 250

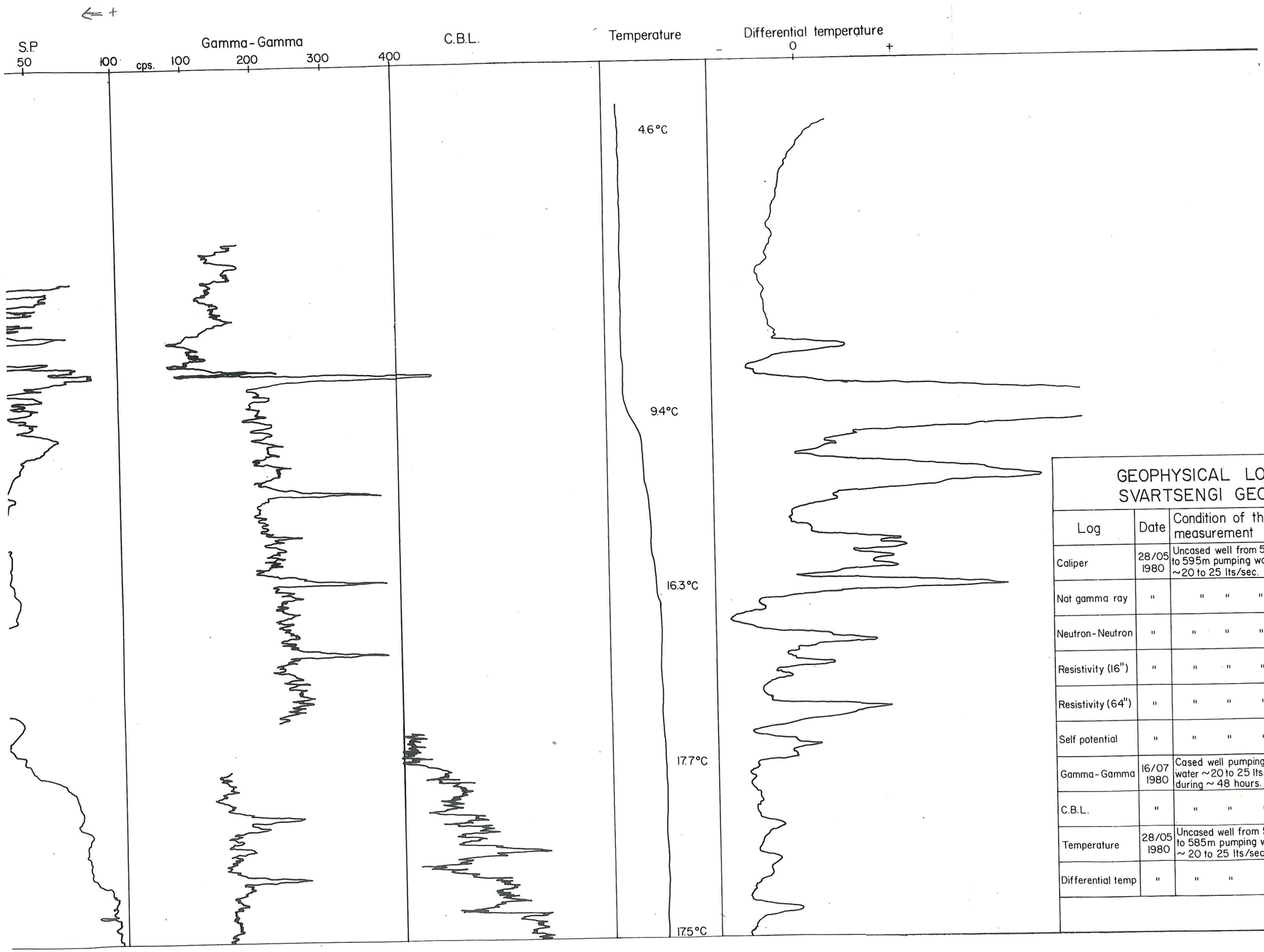

GEOPHYSICAL LOGS - WELL SG-9
SVARTSENGI GEOTHERMAL FIELD.

Log	Date	Condition of the measurement
Caliper	28/05 1980	Uncased well from 57.5 to 595m pumping water ~20 to 25 lts/sec.
Nat gamma ray	"	" " "
Neutron - Neutron	"	" " "
Resistivity (16")	"	" " "
Resistivity (64")	"	" " "
Self potential	"	" " "
Gamma - Gamma	16/07 1980	Cased well pumping water ~20 to 25 lts/sec. during ~ 48 hours.
C.B.L.	"	" " "
Temperature	28/05 1980	Uncased well from 57.5 to 585m pumping water ~ 20 to 25 lts/sec.
Differential temp	"	" " "

Drilling period: 06/02/80 - 22/02/80
28/04/80 - 23/05/80

Depth of the well: 994 m

Drill bits: 22" from 0 to 57.5 m
17 ½" from 55 to 595 m
12 ¼" from 595 to 994 m

Casing diameter: 18 ⅝" from 0 to 57.5
13 ⅜" from 0 to 589.4
Liner diameter: 9 ⅝" from 557 to 976.5

J.L.Z / EBF

DATE

SHEET
N: I.

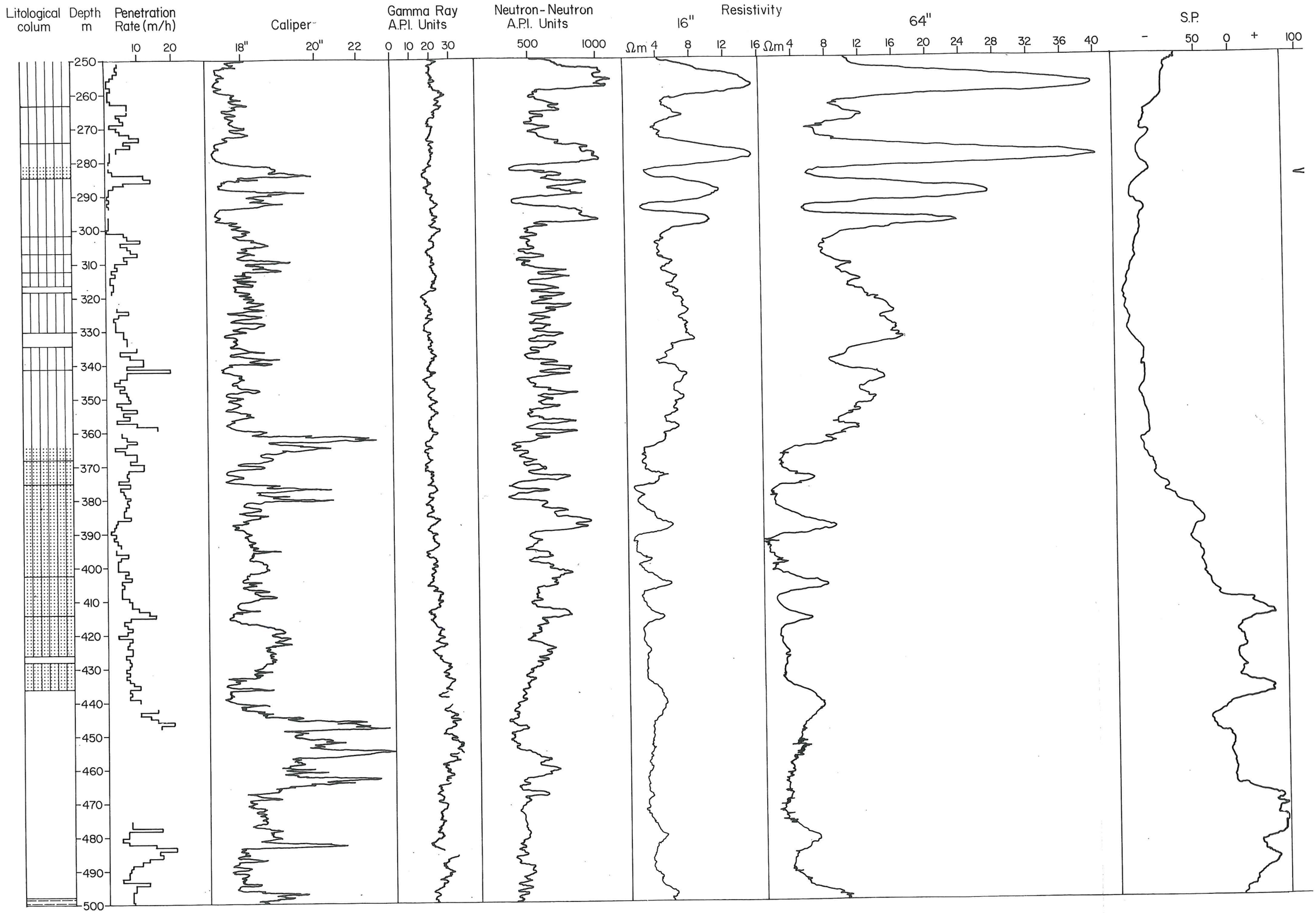
+ →
Litological colum
Depth m
Penetration Rate (m/h)
10 20
Caliper
18" 20" 22
Gamma Ray A.P.I. Units
0 10 20 30
Neutron-Neutron A.P.I. Units
500 1000
Resistivity
16"
Ωm 4 8 12 16
64"
Ωm 4 8 12 16 20 24 28 32 36 40
S.P.
- 50 0 + 100
250 260 270 280 290 300 310 320 330 340 350 360 370 380 390 400 410 420 430 440 450 460 470 480 490 500
V

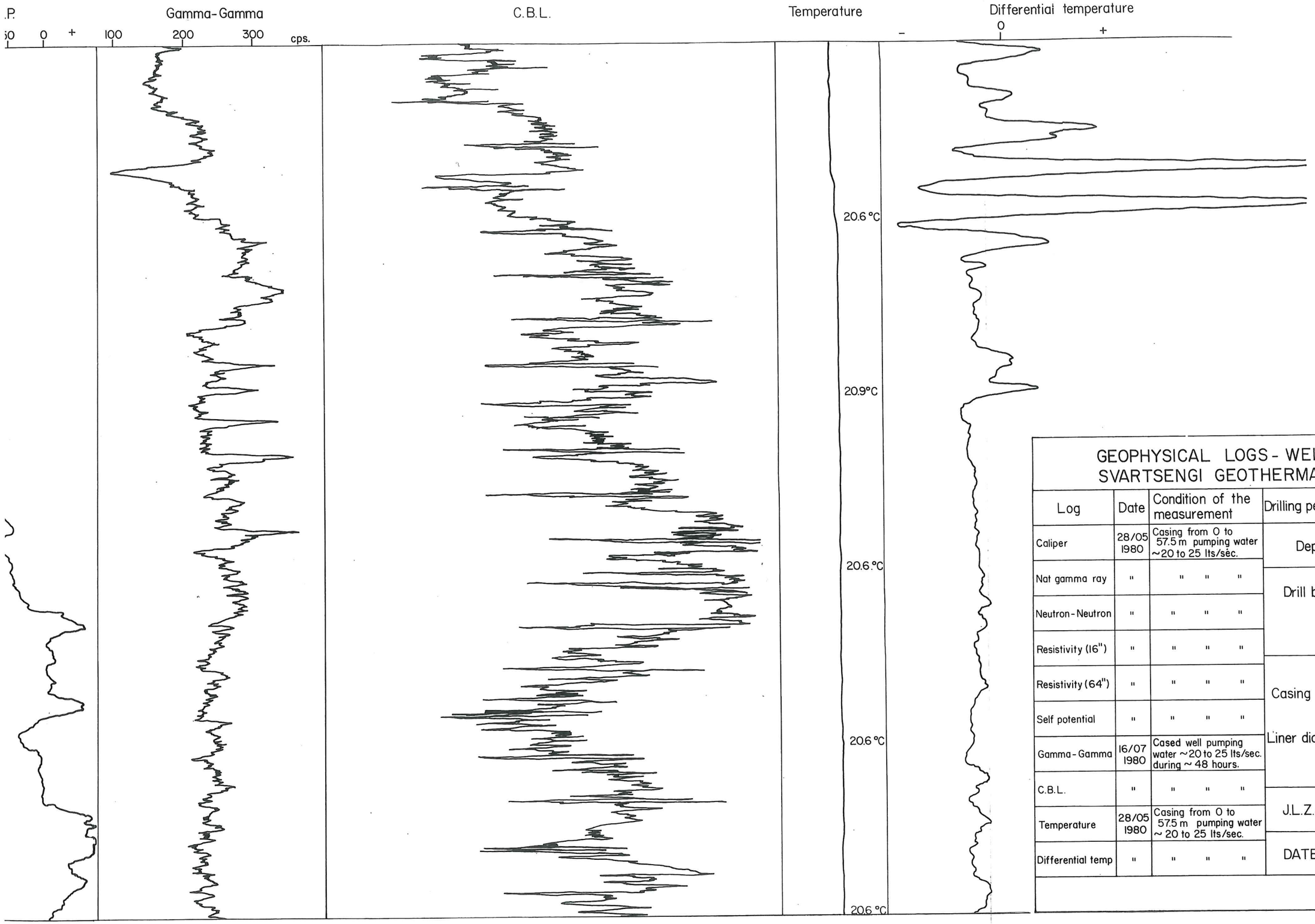

GEOPHYSICAL LOGS - WELL SG-9
SVARTSENGI GEOTHERMAL FIELD.

Log	Date	Condition of the measurement
Caliper	28/05 1980	Casing from 0 to 57.5 m pumping water ~20 to 25 lts/sec.
Nat gamma ray	"	" " "
Neutron - Neutron	"	" " "
Resistivity (16")	"	" " "
Resistivity (64")	"	" " "
Self potential	"	" " "
Gamma - Gamma	16/07 1980	Cased well pumping water ~20 to 25 lts/sec. during ~ 48 hours.
C.B.L.	"	" " "
Temperature	28/05 1980	Casing from 0 to 57.5 m pumping water ~ 20 to 25 lts/sec.
Differential temp	"	" " "

Drilling period: 06/02/80-22/02/80
28/04/80-23/05/80

Depth of the well: 994 m

Drill bits: 22" from 0 to 57.5 m
17 ½" from 55 to 595 m
12 ¼" from 595 to 994 m

Casing diameter: 18 ⅝" from 0 to 57.5
13 ⅜" from 0 to 589.4
Liner diameter: 9 ⅝" from 557 to 976.5

J.L.Z./EBF

DATE.

SHEET N:2.

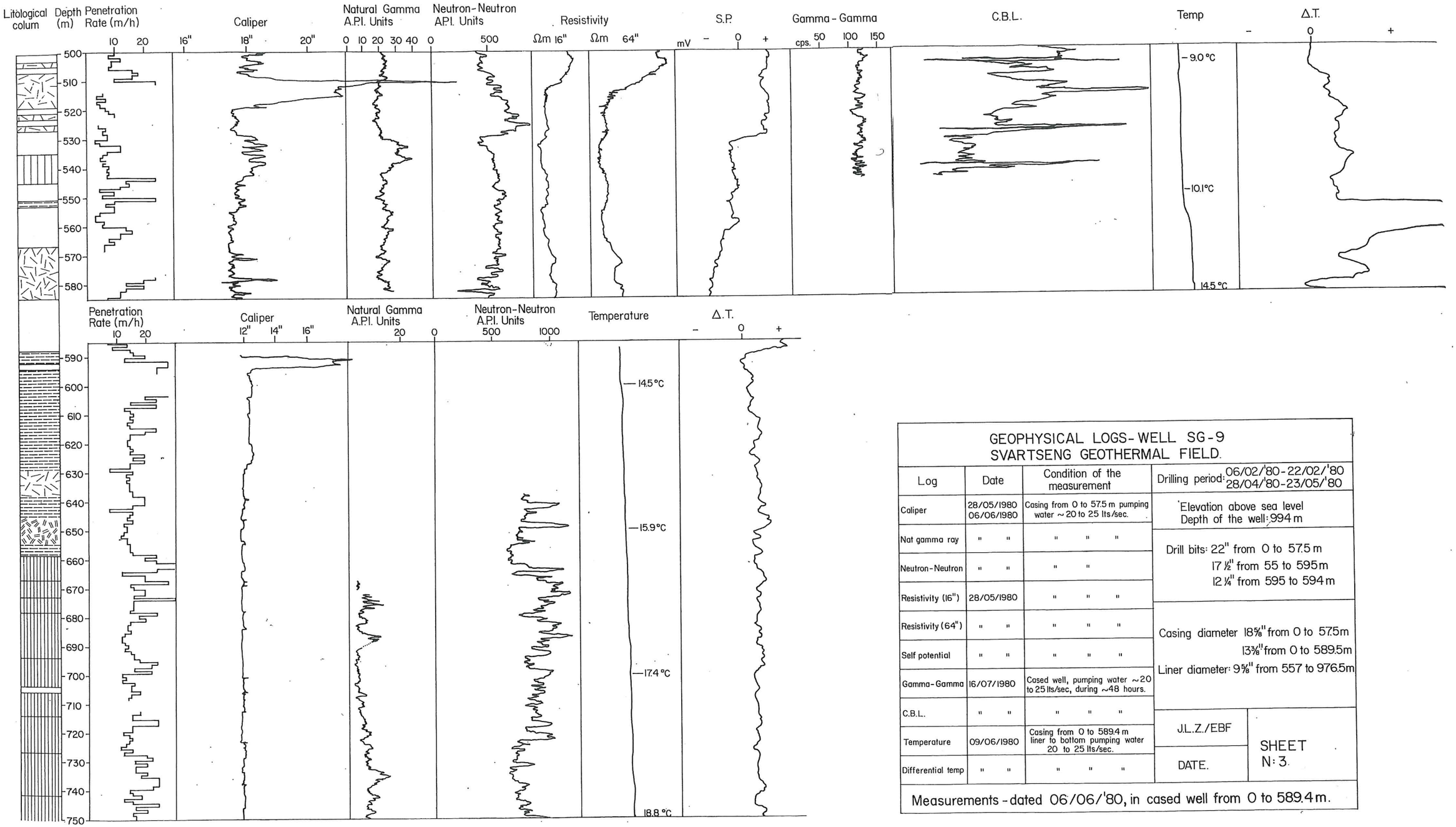

GEOPHYSICAL LOGS - WELL SG-9
SVARTSENG GEOTHERMAL FIELD.

Log	Date	Condition of the measurement
Caliper	28/05/1980 06/06/1980	Casing from 0 to 57.5 m pumping water ~ 20 to 25 lts/sec.
Nat gamma ray	" "	" " "
Neutron-Neutron	" "	" "
Resistivity (16")	28/05/1980	" " "
Resistivity (64")	" "	" " "
Self potential	" "	" " "
Gamma-Gamma	16/07/1980	Cased well, pumping water ~20 to 25 lts/sec, during ~48 hours.
C.B.L.	" "	" " "
Temperature	09/06/1980	Casing from 0 to 589.4 m liner to bottom pumping water 20 to 25 lts/sec.
Differential temp	" "	" " "

Drilling period: 06/02/'80 - 22/02/'80
28/04/'80 - 23/05/'80

Elevation above sea level
Depth of the well: 994 m

Drill bits: 22" from 0 to 57.5 m
17 ½" from 55 to 595 m
12 ¼" from 595 to 594 m

Casing diameter 18⅝" from 0 to 57.5m
13⅜" from 0 to 589.5m
Liner diameter: 9⅝" from 557 to 976.5m

J.L.Z./EBF

DATE.

SHEET N: 3.

Measurements - dated 06/06/'80, in cased well from 0 to 589.4 m.

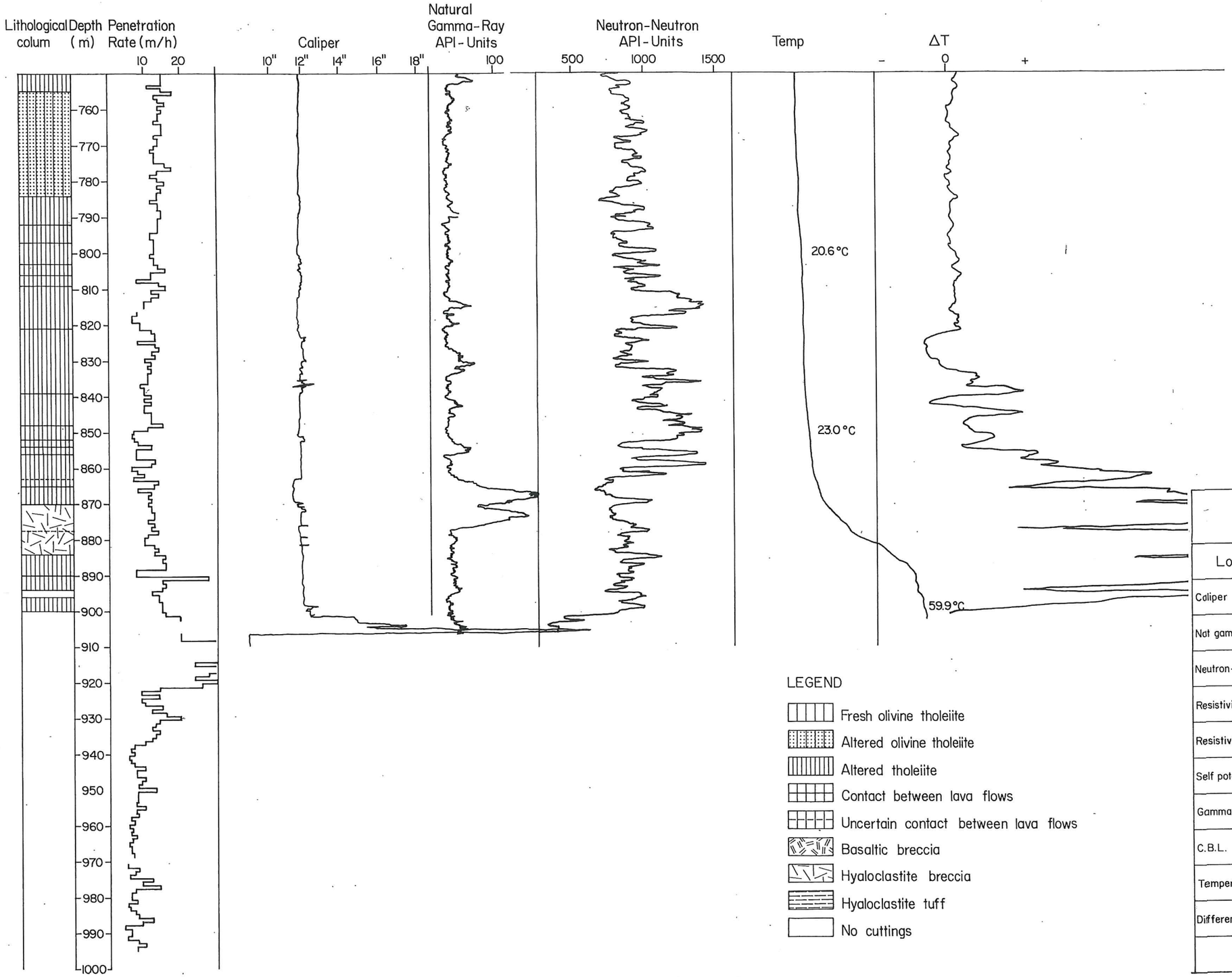

LEGEND

- Fresh olivine tholeiite
- Altered olivine tholeiite
- Altered tholeiite
- Contact between lava flows
- Uncertain contact between lava flows
- Basaltic breccia
- Hyaloclastite breccia
- Hyaloclastite tuff
- No cuttings

GEOPHYSICAL LOGS - WELL SG-9
SVARTSENGI GEOTHERMAL FIELD.

Log	Date	Condition of the measurement
Caliper	06/06 1980	Casing from 0 to 589.4m pumping water ~20 to 25 lts/sec.
Nat gamma ray	"	" " "
Neutron-Neutron	"	" " "
Resistivity (16")		
Resistivity (64")		
Self potential		
Gamma-Gamma		
C.B.L.		
Temperature	09/06 1980	Casing from 0 to 589.4m liner to bottom pumping water ~20 to 25 lts/sec
Differential temp	"	" " "

Drilling period: 06/02/80-22/02/80
28/04/80-23/05/80.

Depth of the well: 994 m

Drill bits: 22" from 0 to 57.5m
17 ½" from 55 to 595m
12 ¼" from 595 to 994m

Casing diameter: 18⅝" from 0 to 57.5
13⅜" from 0 to 589.4
Liner diameter: 9⅝" from 557 to 976.5

J.L.Z./EBF

DATE.

SHEET N:4.